bioRxiv (2023)
doi:10.1101/2021.11.27.470200
a Malthusian Relativity paper

$\iota^{**}=7/3\psi$
mrLife.org

The population dynamic life histories of the birds and mammals of the world

Lars Witting
Greenland Institute of Natural Resources, Box 570, DK-3900 Nuuk, Greenland. email:lawi@natur.gl

Abstract With life history traits determining the natural selection fitnesses of individuals and growth of populations, estimates of their variation are essential to advance evolutionary theory and ecological management during times of global change. As quantitative predictions improve with the completeness of models, and as data are usually incomplete or missing for most species, I use published data and interspecific allometric extrapolations to estimate complete population dynamic life history models for birds and mammals with known body masses. This constructs models for 11,188 species of birds and 4,937 species of mammals, covering 27 life history and ecological traits per species. The estimates are used to illustrate natural selection mechanisms and explain a diverse range of population dynamic trajectories by the inclusion of population dynamic regulation. This provides a first step towards the construction of freely accessible and ready-to-use online population dynamic simulations covering all species of birds and mammals.

Keywords: Life history, population dynamics, natural selection, bird, mammal, allometry

1 Introduction

With life history traits defining the fitness of individuals they provide a gateway to the secrets of natural selection, inspiring evolutionary studies for decades. And with the average fitness of individuals defining the growth of populations, life histories are equally essential for our ability to model and manage the dynamics of natural populations. Improving our skills in both areas are more critical now than ever, as the expanding demands of the growing human population challenge our living planet with climatic change and loss of habitats and biological diversity.

Solutions to the biodiversity and climate crises require political actions. As scientist we can help by integrating biological data into relevant measures, models, and analyses that are freely accessible and easy to interpret and use. This applies not only where data are available, but also by extrapolating our best scientific knowledge for use in critical cases where actions are needed but time and/or economy is too limited for data collection and detailed analysis.

We may use population dynamic data at face value, as in the Living Planet Index (LPI 2022) where timeseries of almost 40,000 populations measure the joint trend in the diversity of animal life on Earth. According to the LPI, vertebrates are on a global retreat with an average decline of about 70% from 1970 to 2018 across all monitored populations. Luckily, the LPI gives a false impression as the estimated decline follows from outliers, with 98.6% of the vertebrate populations across all systems showing no mean global trend (Leung et al. 2020). This highlights the need for species models to analyse the conservation implications of trends, identifying species and regions with need for action, as well as areas that improve.

Population trends have many causes, and their population biological implications are not always as straightforward as they seem. Successful trend analyses depend on realistic population models that can identify the underlying causes of timeseries. With this paper I initiates a project that uses population dynamic timeseries data to estimate first-approximation population dynamic models for all species of birds and mammals with an estimate of body mass. Apart from analysing the underlying causes of existing timeseries, a main goal is the construction of a global library of Bird and Mammal Populations (BMP) that is freely available for online simulations (at https://mrLife.org/bmp.htm). The BMP library allows for population dynamic analyses of all species, including the estimation of expected trajectories given habitats that fragment or improve.

The development of BMP includes three relatively independent stages, with this paper covering the first. Apart from externally imposed variation and trends, the population dynamics of a species is determined by its age-structured demography and population dynamic regulation by density dependent competition and natural selection. While the two regulating forces can be estimated from population dynamic timeseries, these data are generally insufficient for the estimation of the age-structured demography. Hence, in this first stage I

use data from the literature to estimate age-structured life history models for all species with an estimate of mass. Having the age-structure demography I proceed in phase two with the estimation of population regulation for all species with timeseries data of a sufficiently high quality (following the approach in Witting 2021), before the estimates of regulation are extrapolated across species in phase three.

Instead of restricting my estimates to demographic parameters that are necessary for population dynamic simulations, I estimate a much broader set of life history traits where the feeding ecology and energetic physiology of each species are selected in a mutual balance with zero population dynamic growth. Being based on the population dynamic feedback selection of Malthusian relativity (Witting 1997, 2008, 2017a,b), these models have a strong theoretical basic, and a wide range of potential uses including analysis on evolutionary causality (Witting 2023).

1.1 Theoretical foundation

By analysing fitnesses in populations in relation to trade-offs and constraints, the success of classical life history theory (Charlesworth 1980; Roff 1992; Stearns 1992; Charnov 1993) is perhaps best described by it its ability to determine whether a species has evolved to a selection attractor, or not.

At first, this success seems to be somewhat of a paradox. This is because the constant relative fitnesses and frequency-independent selection that is applied in most traditional theory ignores the selection implications of the density and frequency dependent interactions that occur among individuals in natural populations. These interactions are typically competitive, and as they distribute the available resources differentially across individuals, they are directly influencing the relative fitnesses among variants (see e.g. Hardy and Briffa 2013). This makes the relative fitness of a variant dependent not only on the frequencies of the other life history variants in the population, but the frequency dependence is also density dependent as individuals encounter other individuals in competition more often at high population densities. How can a selection theory that does not include these basis rules of competition have any success with evolutionary predictions?

Population dynamic feedback selection takes the alternative game theoretical route (Maynard Smith and Price 1973; Maynard Smith 1982), using asymmetrical interactions (Parker 1974) and Continuously Stable Strategies (Eshel and Motro 1981; Taylor 1989; Christiansen 1991) to analyse life history evolution by the selection of the density-frequency-dependent competitive interactions among individuals in natural populations (including also a subset of trade-offs that cannot evolve). Where most game theory deal with differences in behavioural strategies of competition, population dynamic feedback selection focusses mainly on the interactive asymmetry obtained by life history traits like body mass, group size, the male/female division of labour, and the associated sexual reproduction attraction of two genders. These interactive qualities are inversely related to population dynamic growth by the quality-quantity trade-off (Smith and Fretwell 1974; Stearns 1992), the costs of resource sharing, the two-fold cost of males (Maynard Smith 1971), and the two-fold cost of meiosis (Williams 1975). Their interactive selection is thus controlling the growth, abundance, and level of interference of the population, creating a population dynamic feedback that selects for energetically balanced life histories (Witting 1997, 2002, 2008).

Where classical life history theory often is verified by its ability to mimic fitness distributions in natural populations, feedback selection is tested mainly by its ability to predict evolution in time, including the observed differentiation in life histories among species and higher taxa. This involves *i*) the prediction of life-forms from molecular replicators over prokaryote and protozoa like self-replicating cells to multicellular animals (Witting 2017b), *ii*) the associated prediction of replicating units from asexual replicators over sexually reproducing pairs and cooperative breeders to fully evolved eusocial colonies (Witting 1997, 2002, 2007), and *iii*) the deduction of the inter-specific body mass allometries (Witting 1995, 2017a) that I use in the present paper to extrapolate life history models across birds and mammals.

The difference between the frequency-independent and density-frequency-dependent fitnesses seems to place classical life history theory and population dynamic feedback selection in direct opposition to one another. Yet, it is actually possible to consolidate the two frameworks into a coherent whole by treating the classical method as an instant description of current selection, and population dynamic feedback selection as a description of natural selection through time, including predictions of life history variation between species. This is because the density-frequency-dependence is frozen at instant moments in time, where the population densities and levels of interference are given, and the distribution of variants and relative fitnesses are constant.

The distributions of fitnesses in natural populations at given points in time may thus be analysed relatively

easily by the mathematical framework of constant relative fitnesses to estimate the current outcome of natural selection in relation to the current physiological and ecological trade-offs experience by the species. Yet—as the population density, level of interference, composition of variants, and relative fitnesses start to change with evolution—the frequency-independent framework is usually too rigid for realistic predictions of evolutionary variation across species and time. When attempted, distorted predictions are often obtained (Witting 1997, 2008).

A distortion is evident in allometric theory, where the frequency-independent framework of the metabolic theory of ecology (West et al. 1997, 1999; Brown et al. 2004; Brown and Sibly 2006) predicts an increase in the population dynamic growth rate (r) and carrying capacity (k) with a selection increase in mass (Witting 2018, 2023). These traits, however, are typically not increasing but declining with an increase in mass across natural species (Fenchel 1974; Damuth 1981, 1987), questioning the evolutionary relevance of the metabolic theory of ecology.

By explicitly analysing the selection of density dependent interactive competition, population dynamic feedback selection provides the first and so far only prediction where the inter-specific allometric exponents of the physiological and ecological traits in Table 1 are explained by the natural selection of metabolism and mass (Witting 1995, 2017a), including the observed decline in r and k with a selection increase in mass. This prediction includes not only well-known Kleiber (1932) scaling with typical $\pm 1/4$ and $\pm 3/4$ exponents in terrestrial taxa that forage in predominantly two spatial dimensions, but also corresponding $\pm 1/6$ and $\pm 5/6$ exponents in pelagic species that forage in three spatial dimensions (Witting 1995), and *i*) allometric transitions from prokaryotes to protozoa and multicellular animals (Witting 2017a,b), *ii*) a curvature in the metabolic allometry of placentals (Witting 2018), and *iii*) numerical scaling differences in body mass trajectories of the fossil record predicting biological evolution over millions and billions of years (Witting 2020).

This selection of metabolism, body mass, and allometries follows from a population dynamic feedback where the interactive foraging in overlapping home ranges generates net energy for reproduction, and thus drives the population dynamic growth that determines the population dynamic equilibrium abundance, which in term defines the home range overlap and density dependent level of interference competition that selects net energy into mass, as the larger-than-average individuals monopolise resources during interactive encounters. The selection is defined and constrained by the physiological energetics of individuals, the population dynamic growth, and the resulting foraging ecology where individual opportunities are constrained by the spatial dimensionality of the habitat, the abundance of the population, and the trait-values of the other individuals in the population. This involves a mass-rescaling selection where Kleiber scaling is selected as a secondary response that maintains the net energy of the organism during the selection of mass (Witting 2017a).

It is the life history and ecological traits that are linked to one another in the population dynamic feedback cycle that I estimate in this study. The estimated models are thus directly compatible with the energy flow in population dynamic feedback selection, except that the estimates focus only on the average trait-values, and not on the intra-population differentiation that defines natural selection. For insights on the latter you may consult theoretical studies like Witting (1997, 2002, 2008, 2017a,b).

A main purpose of my paper is to construct the diversity of models that cover the population dynamic life history variation across all species of birds and mammals. Yet, I will also use the intra- and inter-taxa variation of birds, placentals, marsupials, and bats to illustrate that the physiology, demography, and ecology of natural species are selected in a mutual balance that follows the expectations of population dynamic feedback selection. And at the end of the paper, I illustrate how the single species models are easy to extend into simulations that explain a diverse set of population dynamic timeseries by the inclusion of population dynamic regulation.

2 Methods

To estimate the missing life history traits of the different species I combine large datasets published over the past couple of decades with inter-specific extrapolations by allometric correlations reflecting population dynamic feedback selection. Following this method, the minimum requirement for a species model is an estimate of body mass.

To extrapolate life history models across species, I combine the diverse data into a single dataset, and use standard calculations to transform some of the data into common parameters. The data are then checked for outliers and combined with allometric calculations to estimate the missing values for all species with a data-based estimate of body mass.

All of my life history estimates follow the model structure that Witting (2017a,b) used to deduce the

exponents of inter-specific allometries from the natural selection of metabolism, body mass, and the life history and population dynamic foraging ecology as a whole. For a detailed description of the underlying population dynamic feedback selection, you will have to consult these papers, as I restrict myself to the estimation of the underlying population level parameters. Some basic demographic relations are described in Appendix A, with the overall model divided into the four components of individual growth, demography, life history energetics, and population ecology. The four sub-sets of parameters are introduced below.

2.1 Individual growth

The growth of an individual with age (a) is described by

t_p: the gestation period in mammals, and incubation period in birds;

t_0: the age at birth in mammals, and age at hatching in birds, $t_0 = 0$;

t_f: the age at maximum growth, i.e., infliction point;

t_j: the age at weaning in mammals, and age at fledging in birds;

t_d: the age at independence from parents, $t_j \leq t_d < t_m$ with t_m being the age at reproductive maturity, assuming complete parental care for $a < t_d$, and no care for $a \geq t_d$;

w: the average body mass of an adult individual;

w_x: the mass at $t_x = t_0$, t_f, t_j or t_d, with relative mass $\acute{w}_x = w_x/w$.

Embryotic growth from age $-t_p$ to t_0 is calculated by the Gompertz (1832) growth curve, following the regularities estimated by Ricklefs (2010), where the asymptote ($\acute{w}_\infty$) of the Gompertz growth function $\acute{w}_a = \acute{w}_\infty e^{-be^{-ka}}$ is 2.5 times $\acute{w}_0$ for embryotic growth, and the growth rate $k = 1.9t_p^{-0.9}$ is approximately inversely proportional to the gestation/incubation period. This implies the following embryotic growth

$$\acute{w}_a = 2.5\acute{w}_0 e^{\ln[0.4\acute{w}_p/\acute{w}_0]e^{-1.9t_p^{-0.9}(a+t_p)}} \quad (1)$$

with age $-t_p \leq a < 0$ given in days and relative mass at $-t_p$ being $\acute{w}_p = e^{(e^{1.9t_p^{0.1}}-1)\ln 0.4 + \ln \acute{w}_0}$.

Growth after birth/hatching is estimated by the Richards (1959) growth function, with species specific data-estimates of the inflection point obtained by least-square fitting to growth data obtained from the literature [supplementary information (SI) on inflection]. The growth function

$$\acute{w}_a = \frac{\acute{w}_0}{[\acute{w}_0^z + (1-\acute{w}_0^z)e^{-ka}]^{1/z}} \quad (2)$$

passes through $\acute{w}_0$ at $a = t_0 = 0$ and $\acute{w}_j$ at $a = t_j$, with $k = -\ln[\acute{w}_0^z(\acute{w}_j^{-z} - 1)/(1-\acute{w}_0^z)]/t_j$ and a relative adult mass of unity ($\acute{w}_\infty = 1$). The infliction point $\acute{w}_f$ relative to adult mass is calculated given the fitted or extrapolated estimates of the shape parameter z, with $\acute{w}_f$ increasing from zero to 0.5 when z increases from -1 to 1.

There is only little information available on t_d and $\acute{w}_d$ (but see e.g. Millar et al. 1986; Lloyd 1987; Johansson et al. 2021). While I treat independence as a knife-edge parameter, real independence is a gradual development. Independence is often quite late compared to weaning in mammals, and often quite close to fledging in birds [with median $\acute{w}_j$ being 0.33 (cv:0.77) and 0.84 (cv:0.24) in mammals and birds for the data in the present study]. With no clear data estimates, I assume that parents invest at least 80% in the mass of offspring (either directly, or indirectly by protecting the foraging area of offspring). The relative mass at independence is thus $\acute{w}_d = \max(\acute{w}_j, 0.8)$, with t_d being the solution to eqn 2 at $\acute{w}_d$.

2.2 Demography

The demographic traits include

p_{ad}: the annual survival probability of adults (geometric mean across adult age-classes);

q_{ad}: the annual mortality of adults, $q_{ad} = 1 - p_{ad}$;

t_s: female age at sexual maturity;

t_m: female age at reproductive maturity, $t_m = t_s + t_p$;

t_r: the expected reproductive period for females that survive to t_m, estimated as $t_r = 1/q_{ad}$ by eqn 12;

t_g: generation time as the average age of reproduction, as $t_g = t_m + p_{ad}/q_{ad}$ by eqn 14;

t_l: the maximum lifespan of an individual;

l_m: the probability that a new-born survives to t_m, as $l_m = 2/R$ by eqn 3;

l_r: the probability that an adult survives the expected reproductive period, $l_r = {p_{ad}}^{t_r}$;

	w	w_0	w_j	w_f	β	$\underline{\beta}$	t_p	t_j	t_s	t_m	t_l	m_b	m_f	m_i	p_{ad}	N	h
Ave.	11188	774	207	155	76	470	2237	1819	1210	681	1667	6979	1765	0	908	1438	249
Mam.	4937	1868	1059	101	57	713	2217	2040	1999	935	2614	3511	2146	651	310	1111	456

	w	β	t_x	m	R	l_m	l_r	ϵ	α	N	b	ϵ_n	h	h_o	I
Exp.	1	$-\frac{1}{2d}$	$\frac{1}{2d}$	$-\frac{1}{2d}$	0	0	0	$\frac{2d-1}{2d}$	1	$\frac{1-2d}{2d}$	$\frac{1}{2d}$	0	1	$\frac{1}{2d}$	0

Table 1: Top table: The number of birds (Ave) and mammals (Mam) with data estimates across traits. Bottom table: The body mass allometry exponents predicted by population dynamic feedback selection; see mathematical deductions in Witting (1995, 2017a) or graphical deduction in Witting (2023) [$t_x \in \{t_p, t_j, t_s, t_m, t_r, t_g, t_l\}$]. These exponents depend on the ecological packing of home ranges in one, two, or three spatial dimensions (d), as listed in Table 2.

Class	Order	Family	d
Aves	-	-	2
Mammalia	-	-	2
Mammalia	Primates	-	3
Mammalia	Carnivora	-	2
Mammalia	Carnivora	Otariidae	3
Mammalia	Carnivora	Odobenidae	3
Mammalia	Carnivora	Phocidae	3
Mammalia	Cetacea	-	3

Table 2: The spatial dimensionality (d) of the ecological packing of home ranges is set to depend on taxonomic level, following the classification in Witting (2017a).

m**:** the average number of offspring produced per female per year, i.e., $m = m_b\, m_f$ where m_b is the average brood size and m_f the average brood frequency, with m_f being the inverse $m_f = 1/m_i$ of the average brood interval m_i; and

R**:** expected lifetime reproduction as the average number of offspring produced over the expected reproductive period of females that survive to t_m, estimated as $R = t_r m$.

These parameters are estimated for species that are assumed to be naturally selected around a population dynamic equilibrium with a per-generation growth rate of unity

$$\lambda = l_m t_r m/2 = 1, \tag{3}$$

assuming an even sex ratio.

2.3 Life history energetics

Traits that link the demographic parameters to the energetics of the organism include

w_ϵ**:** body mass as combustion energy (SI unit J); obtained as $w_\epsilon = c_{w\to d} c_{d\to\epsilon} w$, with w being mass in grams, $c_{w\to d}$ the conversion of wet organic matter to dry [0.40 for birds (Mahoney and Jehl 1984), and 0.35 for mammals (Prothero 2015)], and $c_{d\to\epsilon}$ the conversion of dry matter to energy [22.6 kJ/g from Odum et al. (1965) and Griffiths (1977)];

$\underline{\beta}$**:** basal mass-specific metabolism (SI unit W/g);

β**:** field mass-specific metabolism (SI unit W/g) also the pace (SI unit Hz) of the metabolic work carried out per unit body mass;

α : the handling of net resource assimilation (resource handling in short, SI unit J), defined as the net energy that is generated per metabolic pace (estimated as $\alpha = \epsilon/\beta$). Handling is a joint parameter ($\alpha = \grave{\alpha}\rho$) of intrinsic handling ($\grave{\alpha}$) multiplied by the density of the resource (ρ);

ϵ**:** the net assimilated energy of adults is the product ($\epsilon = \alpha\beta$; SI unit W) of resource handling (α) and metabolic pace (β). Following the selection attractor of sexually reproducing pairs (Witting 2002), half of the join net energy (2ϵ) of the female/male unit is allocated to reproduction, while the other half is used in intra-specific interactions. Net energy is estimated as $\epsilon = w_e \acute{\beta} R/t_r$ from eqn 4; and

ϵ_g**:** average gross energy $\epsilon_g = w\beta + \epsilon/2$ (SI unit W; given as a relative measure $\acute{\epsilon}_g = \epsilon_g/\epsilon$) is total field metabolism plus net energy allocated to reproduction. The latter is $\epsilon/2$ as the reproducing unit uses half of their net energy in reproduction, while the other half that is used in intra-specific interactions is included here in average field metabolism.

Net energy defines lifetime reproduction by the number of fully growth offspring that it produces. Assuming complete parental investment until t_d, we have

$$R = \epsilon t_r / \acute{\beta} w_\epsilon \tag{4}$$

where

$$\acute{\beta} = (w_d + t_e \beta \bar{w}_d)/w \quad (5)$$

is a scaling parameter that scales w_ϵ to the mass at independence (w_d) and accounts for the energy that is metabolised by the offspring during parental care ($t_e = t_p + t_d$), with $t_e \beta \bar{w}_d$ being the energy that is metabolised by the offspring during t_e, assuming constant mass-specific metabolism (β) and an average size

$$\bar{w}_d = \frac{1}{t_e} \int_{a=-t_p}^{t_d} w_a \, da \quad (6)$$

that is calculated by the growth model of eqns 1 and 2, with $-t_p$ being the negative age at fertilisation.

2.4 Population ecology

Important population ecological components include

N**:** population density (abundance), as the number of animals per km^2;

b**:** the standing biomass of the population, as $b = wN$ in kg/km^2;

ϵ_n**:** the energy consumed by the population, calculated as $\epsilon_n = \epsilon_g N$ (in W/km^2);

h**:** the average home range of an individual (in km^2);

h_o**:** the average home ranges overlap $h_o = hn$, given as home range divided by the available of space ($1/N$) per individual;

v**:** the frequency of competitive encounters per individual per unit home range overlap, given as a relative measure $v \propto v_f/l_f$, where $l_f \propto h^{1/d}$ is the length of foraging tracks (proportional to the dth root of the home range in d-dimensions) and $v_f \propto \beta_\beta w^{1/2d}$ the average foraging speed obtained from allometric correlations where β_β is the intercept of the metabolic allometry $\beta = \beta_\beta w^{-1/2d}$ (Witting 1995, 2017a); and

I**:** intra-specific interference competition per individual, calculated as a relative measure $I \propto h_o v \propto Nhv$ from the overlap in home ranges and the frequency of encountering other individuals per unit home range overlap (Witting 1995, 2017a). These I estimates are rescaled for a log value ($\iota = \ln I$) of unity at the median across all species of birds.

2.5 Data

My study extends on the data used by Witting (2023), with all literature estimates treated as raw data. My broad definition of data includes the traits of a species that are calculated from the raw data of that species.

I use the BirdLife (2022) taxonomy for birds, and MDD (2023) taxonomy for mammals, with some subspecies with separate body mass estimates categorised as species. Body mass data were obtained from several sources including Smith et al. (2004), Dunning (2007), Jones et al. (2009), Weisbecker et al. (2013), Myhrvold et al. (2015), Tobias et al. (2021), and Herberstein et al. (2022). Demographic parameters on reproduction, time periods, and growth were achieved from many datasets including Jetz et al. (2008), De Magalhães and Costa (2009), Jones et al. (2009), and Myhrvold et al. (2015), with growth curve data and survival rates obtained from an independent literature search, including survival estimates from McCarthy et al. (2008), DeSante and Kaschube (2009), Ricklefs et al. (2011), del Hoyo et al. (1992–2011), and Wilson and Mittermeier (2009–2014). Ecological parameters included population densities from Damuth (1987) and Santini et al. (2018), and home range areas from Tucker et al. (2014), Tamburello et al. (2015), and Nasrinpour et al. (2017) with an independent literature search for marine mammals and bats. Basal metabolic rates were obtained primarily from McNab (2008) for mammals and from McKechnie and Wolf (2004) for birds, with field metabolism for both taxa provided by Hudson et al. (2013).

Altogether, 110,105 trait values were obtained from 614 literature sources. Some of these data are the same, and I put more weight on commonly agreed estimates by using the average trait values of the available raw data for each trait per species. This resulted in 58,548 species specific raw data, with Table 1 listing the number of species with raw data for different traits.

These data are distributed relatively evenly across the taxonomic groups considered separately in this paper. For the traits in Table 1, there were on average raw data for 17% of the bird species and 23% of the mammalian species, with the latter including 25% for placentals, 31% for marsupials, and 15% for bats. These data, except for body mass estimates, were checked for outliers (see outlier SI), with a total of 474 outliers removed.

I list the literature references for all raw data (follow the letter codes in the SI on estimates and SI on data references), and for the underlying raw data when derived traits are calculated from one or two underlying traits with raw data estimates. Higher-level data

	w_0	w_j	β	$\underline{\beta}$	t_m	t_l	t_p	t_j	m	p_{ad}	q_{ad}	N	h
q_g	3.53	4.61	0.16	3.99	3.39	0.05	2.60	0.08	3.39	0.06	0.26	0.81	0.26
q_n	8.1	10.7	30.6	27.0	17.5	100.0	19.0	46.5	29.9	54.6	19.0	83.9	28.0
q_x	0.33	0.33	1.05	1.02	0.47	0.78	0.33	0.51	0.33	0.42	0.85	0.62	0.99
$\hat{x}$	−0.34	−0.15	−0.16	−0.11	0.02	0.16	0.03	0.14	0.06	−0.11	0.09	−0.34	0.95
σ	0.47	0.71	0.79	0.65	0.98	1.18	0.39	0.58	1.05	1.05	1.22	3.98	3.45
$\hat{x}$	−0.30	−0.12	−0.26	−0.27	0.13	0.13	0.07	0.15	−0.08	0.08	−0.14	−0.39	0.86
σ	0.32	0.54	0.29	0.27	0.39	0.77	0.20	0.28	0.60	0.25	0.44	1.44	1.98
$\hat{x}$	−0.20	−0.13	−0.29	−0.30	0.24	0.21	0.13	0.20	−0.16	0.10	−0.23	−0.37	0.92
σ	0.30	0.43	0.20	0.22	0.37	0.47	0.10	0.17	0.80	0.07	0.24	0.56	0.89
$\hat{x}$	−0.16	−0.09	−0.33	−0.31	0.22	0.22	0.18	0.24	−0.16	0.08	−0.21	−0.55	1.06
σ	0.06	0.05	0.03	0.06	0.01	0	0	0.03	0.02	0	0.01	0.16	0.03
cv	0.14	0.15	0.14	0.12	0.14	0.24	0.05	0.09	0.13	0.12	0.21	0.87	1.04
n	2117	985	682	644	2446	3526	3653	3133	3112	695	695	1742	337
cv	0.24	0.21	0.15	0.15	0.20	0.25	0.11	0.18	0.23	0.17	0.25	0.95	1.12
n	459	227	477	462	507	629	728	647	624	376	376	712	289
cv	0.38	0.25	0.23	0.20	0.24	0.31	0.20	0.31	0.30	0.20	0.35	1.38	1.35
n	50	45	66	67	46	45	61	57	58	69	69	49	42
cv	2.26	0.26	0.33	0.26	0.48	0.33	0.12	0.52	0.25	0.10	0.32	1.04	2.70
n	6	7	9	9	5	5	4	2	2	7	7	12	8

Table 3: **Missing value estimation.** The q_g, q_n and q_x parameters of eqns 8 and 9 that give the most precise estimation of missing values for the different mass-dependent traits. $\hat{x}$ is the average, and σ the standard deviation, of the data estimated allometric exponents at the different taxonomic levels (blue:genus; green:family; yellow:order; red:class). The precision of an estimated missing value is given by a coefficient of variation (cv) that is estimated from the missing value predictions of n data points.

that are calculated from more traits are listed as data but with no specific reference. Traits that could not be calculated from the raw data of a species had missing values that were estimated by inter-specific extrapolations.

2.6 Estimating missing values

I estimated missing values by inter-specific body mass allometries and invariances following the allometric model of Witting (2017a), using the estimation sequence in Appendix B.

Estimation level: As my data come from many different sources, and as they have not been collected as a random sample across the different species, they are phylogenetically unevenly distributed. This means that the uncertainties of the missing value estimates will increase with the phylogenetic distance to the nearest species with data. To capture this uneven distribution of uncertainties, I use a missing parameter estimator that differentiates between the different phylogenetic levels. This provides separate estimates of uncertainty for the different parameters at the different phylogenetic estimator levels. The uncertainty distribution is visualised for all parameter estimates across all species by a colour code, where data are presented in black and missing parameter estimates at the genus, family, order, and class levels are presented in blue, green, yellow, and red.

Missing values were estimated at the different taxonomic levels dependent upon the available data. The precision of an allometric estimate will generally increase with the number of data and decline with taxonomic level from genus over family and order to class. With the number of data points for any trait increasing with taxonomic level, we expect a trade-off where an estimator based on few data at a low taxonomic level will, at some point, provide a better estimate than an estimator with many data at a higher taxonomic level.

To determine the data limits—where lower-level estimators are preferred over higher-level estimators with more data—I constructed a hierarchical estimator that used the lowest taxonomic level with a given number (n_d) of data points. This number was estimated by a numerical minimization of the sum of squares of the difference between raw data and their predicted values, with the predicted data values of a species being predicted from the raw data of all other species.

Given the optimal missing value estimation of eqns 7 to 9 below, the minimization of the sum of squares between the raw data and their predicted values determined that the more precise estimates of missing values were obtained with a n_d parameter around unity. Taxonomic proximity was thus prioritized over sample size, with missing values being calculated at the lowest tax-

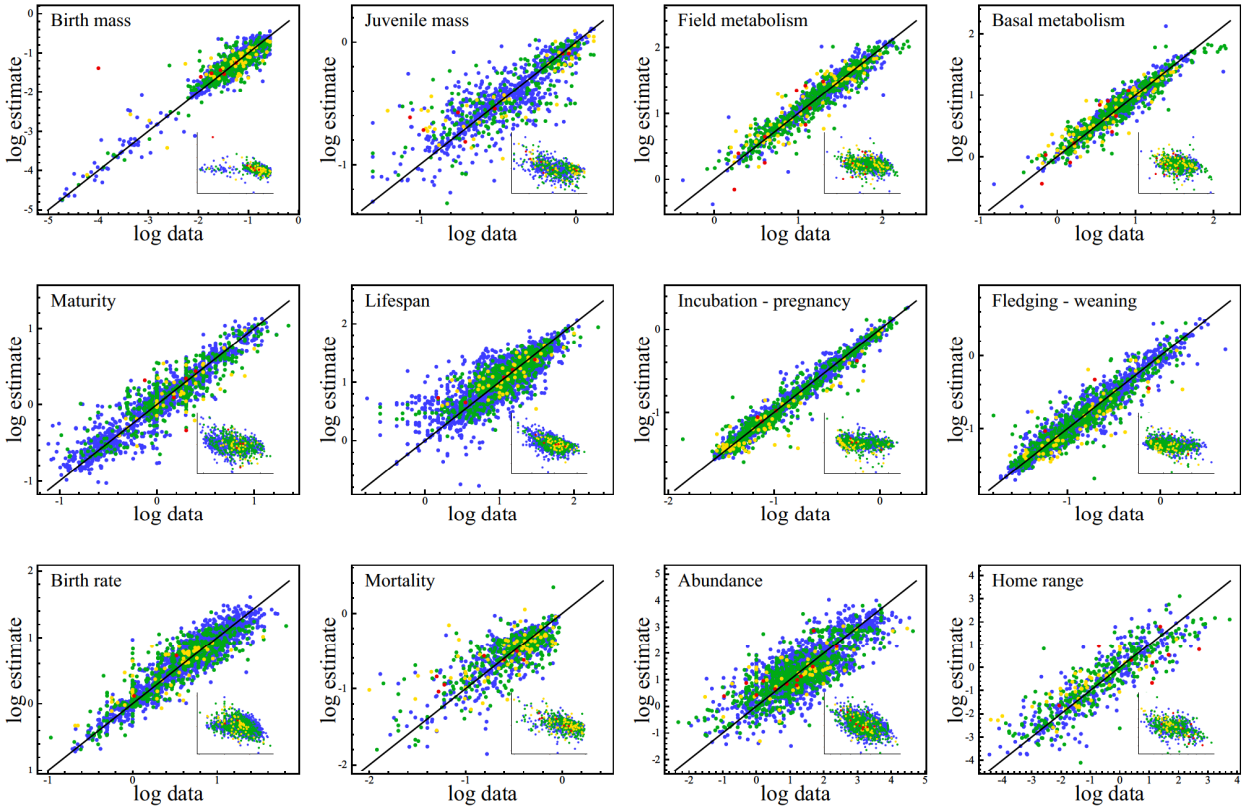

Figure 1: **Data estimation.** The estimation of missing parameters by allometric correlations was cross-validated and optimised by the ability to predict the actual data; as illustrated here by the relationships between the data and their estimates on double logarithmic scale. Residuals are shown in insert plots, and the precision (cv) of the estimates are given in Table 3. Estimator levels: genus (blue), family (green), order (yellow), and class (red); with points of the latter sitting on top of the former.

onomic level with one or more raw data of the required parameters. Genus (g) was prioritized over family (f), family over order(o), and order over class (c).

Estimator optimisation: The missing values of mass-dependent parameters were calculated as allometric functions of mass. The age of reproductive maturity, e.g., was calculated as

$$t_m(x,n) = t_{m,\circ} w^{\hat{t}_m} \tag{7}$$

with x denoting the lowest taxonomic level with raw data, and n the number of data points at that level. The allometric exponent ($\hat{t}_m$) and intercept ($t_{m,\circ}$) were estimated as a joint function

$$\begin{aligned} \hat{t}_m &= q\,\hat{t}_{m,D} + (1-q)\,q_x \hat{t}_{m,T} \\ t_{m,\circ} &= q\,t_{m,\circ,D} + (1-q)\,t_{m,\circ,T} \end{aligned} \tag{8}$$

of the theoretical expectations from Witting (1995, 2017a) [subscript T; e.g. $\hat{t}_{m,T} = 1/2d$ from Table 1 with ecological dimensionality (d) from Table 2] and the n data points at the xth taxonomic level [subscript D, with $\hat{t}_{m,D}$ and $t_{m,\circ,D}$ being point estimates from a linear regression on double logarithmic scale]. The weight

$$q = 1 - e^{-e^{-q_g(n-q_n)}} \tag{9}$$

of the data estimate increases monotonically from zero to one as a function of n, except for $n \leq 3$ cases where the exponent ($\hat{t}_m = q_x \hat{t}_{m,T}$) was proportional to the theoretical expectation and the $t_{m,\circ}$ intercept of eqn 7 was the average allometric intercept for the n species given the $\hat{t}_m$ exponent. Having no theoretical expectation for $\acute{w}_0$ and $\acute{w}_j$, their theoretical values were replaced with exponents estimated by linear regression across all raw data for birds, placentals (minus bats), marsupials, and bats (estimates varying from -0.07 to 0.22).

The three parameters q_g, q_n, and q_x were estimated separately for all mass dependent parameters. This

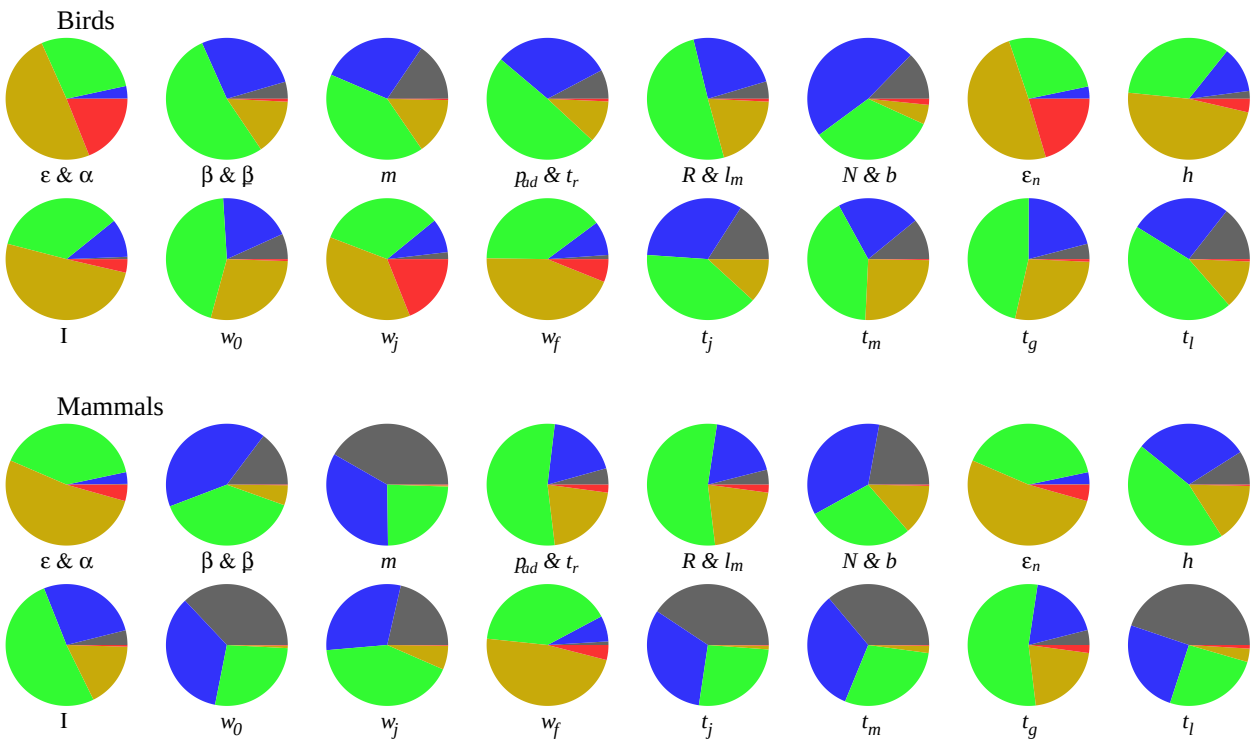

Figure 2: **Estimator distributions** for 11,188 species of birds, and 4,937 species of mammals. Estimator levels: data (black), genus (blue), family (green), order (yellow), and class (red).

was done by a numerical minimization of the sum of squares (across species with data) of the difference between their raw data and the predicted values by the estimators at the lowest taxonomic levels, given the data of all the other species.

Invariance estimators were used only for lifetime reproduction (R) and the inflection parameter z. These were estimated as the average of the data across the lowest taxonomic level with data for that parameter.

Given estimators at the lowest taxonomic level with data, the optimal values of the parameters for eqns 8 and 9 are listed in Table 3. They follow a general pattern where missing parameters are calculated from the theoretical exponents for estimators with few available data. With an increased number of data there often is a steep transition to a fully empirically based estimator, with the average values of the empirically estimated exponents listed in Table 3, for estimators at the genus (blue), family (green), order (yellow), and class (red) level.

The average precision (cv) of the missing parameter estimates are also listed in Table 3. Excluding the estimator for abundance (N) and home range (h), the precisions are generally acceptable for all estimators. The average cv is 0.23, with a range that varies from 0.05 to 2.70. Precision is generally declining with the taxonomic level of the estimator, with the average cv being 0.20 at the genus level, 0.32 at the family level, 0.41 at the order level, and 0.77 at the class level.

A cross validation, which shows how well the different raw data points are predicted by the inter-specific extrapolations that exclude the estimated data points, is shown in Fig. 1. There is a close to linear dependence for all traits, yet some traits tend to be overestimated for small masses (see e.g. residual plots for juvenile mass and abundance).

3 Results

3.1 Estimation level & space

Fig. 2 shows the proportions of estimation levels for the different parameter. Mammals have a larger fraction of data than birds for most traits, yet even for birds 85%, 93%, 92%, 88%, 74%, and 86% of the estimates for m, N (and b), t_p, t_j, t_m and t_l are at or below the family

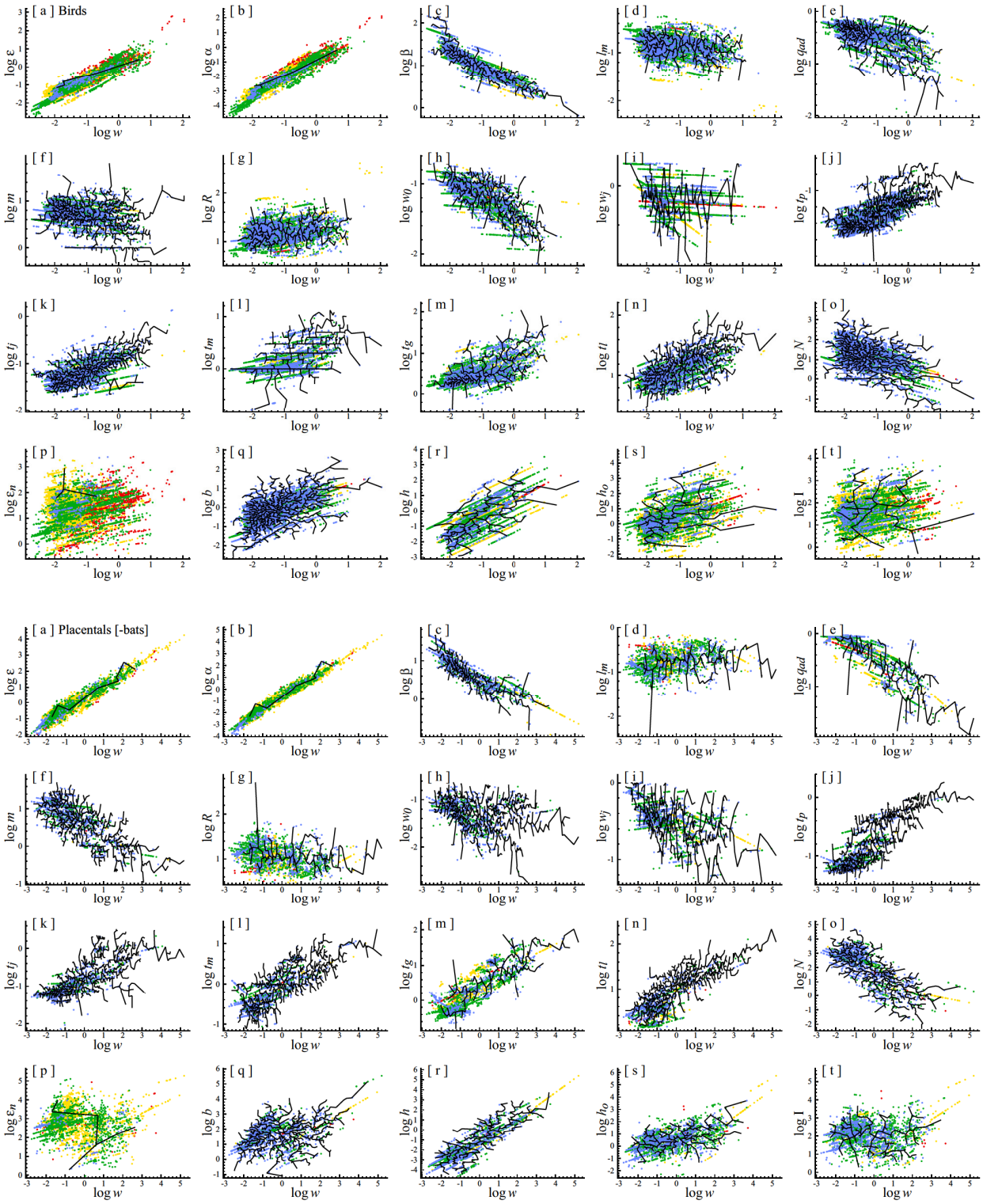

Figure 3: **Allometric scaling.** Birds in the top four rows, placentals (minus bats) in the bottom four. The non-overlapping black lines connect data, and the coloured dots are estimates at different levels. Estimator levels: data (black), genus (blue), family (green), order (yellow), and class (red); with points of the latter sitting on top of the former.

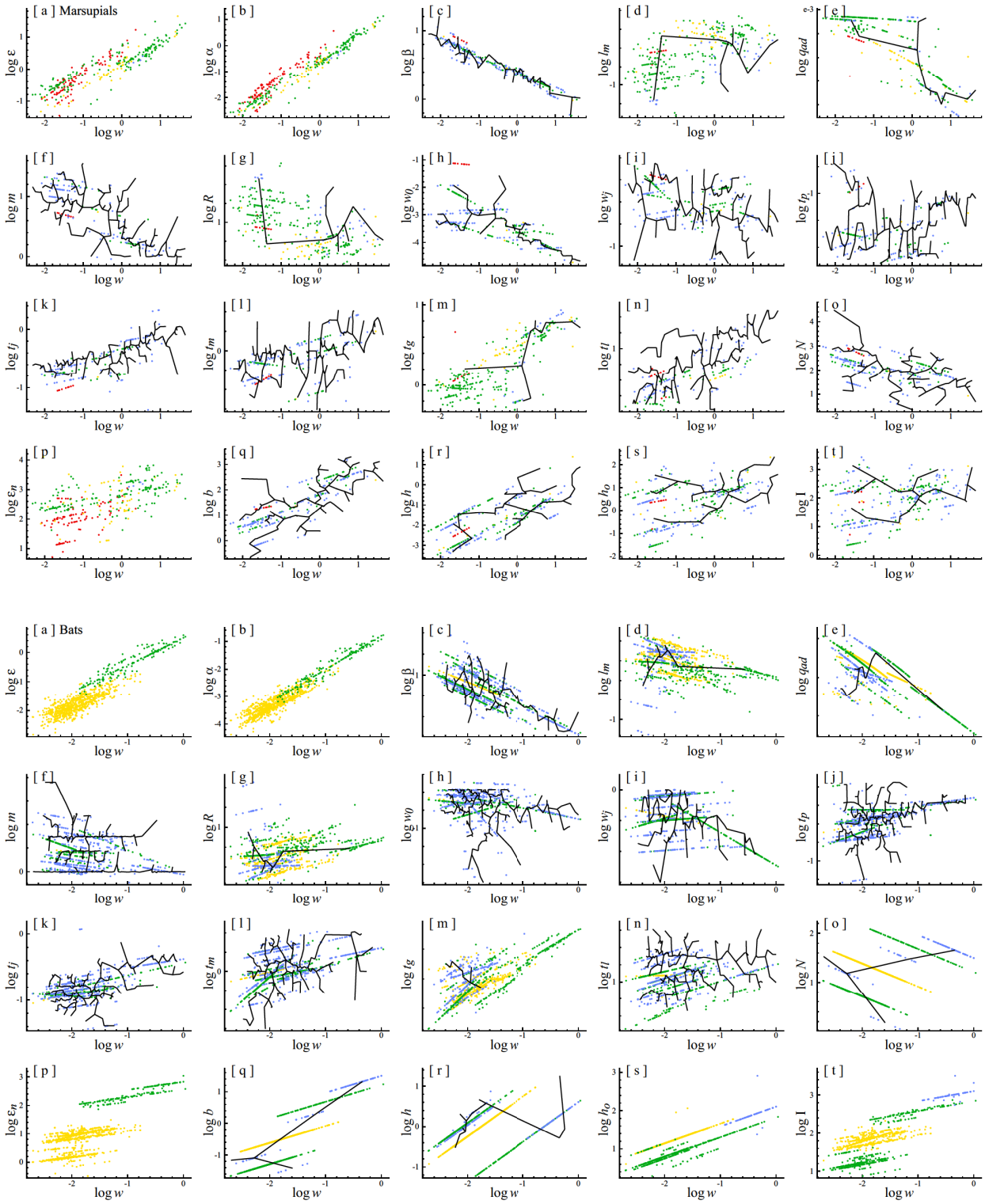

Figure 4: **Allometric scaling.** Marsupial mammals in the top four rows, bats in the bottom four. The non-overlapping black lines connect data, and the coloured dots are estimates at different levels. Estimator levels: data (black), genus (blue), family (green), order (yellow), and class (red); with points of the latter sitting on top of the former.

Trait	w	w_0	w_j	w_f	z	t_p	t_j	t_m	t_r	t_g	t_l	l_m	p_{ad}	m	R
Unit	kg	-	-	-	-	y	y	y	y	y	y	t_m^{-1}	y^{-1}	y^{-1}	t_r^{-1}
Striped Bandicoot *Microperoryctes longicauda*	$^{a:c:d:wq:ws}$ .53	.00039	.2	.37	.029	.034	.15	.35	4.5	3.8	4.8	.49	.78	.91	4.1
Bunyoro Rabbit *Poelagus marjorita*	$^{a:c:d}$ 2.5	.038	.25	.4	.16	$^{c:d}$ .098	.077	.7	1.6	1.3	8.1	.15	.37	8.6	14
Nelsons Spiny Pocket Mouse *Heteromys nelsoni*	$^{a:c:d}$ .063	.047	.51	.52	1.3	.075	.076	.45	1.3	.75	1.8	.23	.24	6.8	8.8
Lesser Egyptian Jerboa *Jaculus jaculus*	$^{a:c:d:e}$ .057	$^{c:d}$ .034	^{d} .35	.46	.61	$^{c:d}$ .098	$^{c:d}$ .16	$^{c:e}$ .86	1.5	1.4	^{d} 7.3	.28	.33	$^{c:d:e}$ 4.7	7.1
Ash-gray Mouse *Pseudomys albocinereus*	$^{a:c:d}$ .03	.076	^{d} .58	.46	.61	$^{c:d}$ .088	$^{c:d}$ .082	$^{c:d}$ .3	1.2	.47	^{d} 2.7	.19	.14	$^{c:d}$ 8.8	10
Hoffmanns Sulawesi Rat *Rattus hoffmanni*	^{a} .15	.027	.32	.46	.61	.062	.069	.31	1.1	.44	3.3	.075	.12	24	27
Small-footed White-toothed Shrew *Crocidura parvipes*	-	-	-	-	-	-	-	-	-	-	-	-	-	-	-
Sri Lankan Shrew *Suncus fellowesgordoni*	^{d} .0023	^{d} .088	^{d} .89	.53	1.4	^{d} .076	^{d} .055	^{d} .7	1.1	.84	^{d} 3.2	.13	.12	^{d} 13	15
Guinean Horseshoe Bat *Rhinolophus guineensis*	^{d} .012	.17	.94	.56	1.7	^{d} .33	^{d} .17	1.7	3.8	4.5	11	.49	.74	1.1	4.1
Ryukyu Long-fingered Bat *Miniopterus fuscus*	$^{a:d}$ .011	^{d} .26	^{d} 1	.56	1.7	^{d} .27	^{d} .18	^{d} 1.9	3.9	4.8	^{d} 22	.52	.74	.98	3.8
Chocolate Pipistrelle *Hypsugo affinis*	^{d} .0084	.19	.69	.56	1.7	.2	.15	.8	3.2	3	4	.27	.69	2.3	7.5
Long-tailed Pangolin *Phataginus tetradactylus*	$^{a:c:d}$ 2.5	.075	$^{c:d}$ .17	.42	.3	.35	.49	2.5	6	7.5	8.5	.32	.83	$^{c:d}$ 1.1	6.3
Nyala *Tragelaphus angasii*	$^{a:c:d:e}$ 99	$^{c:d}$ .058	.2	.48	.76	$^{c:d}$ .61	$^{c:d}$ .58	$^{c:e}$ 1.6	7.3	7.9	^{d} 19	.23	.86	$^{c:d:e}$ 1.2	8.8
Western Ornate Fruit-dove *Ptilinopus ornatus*	$^{b:d:wq}$ .11	.059	.82	.46	.61	.051	.036	.68	2.4	2.1	13	.18	.58	4.7	11
Ashy Woodpecker *Mulleripicus fulvus*	^{b} .31	.029	.81	.47	.73	.042	.083	1	3.3	3.3	13	.1	.7	5.8	19
Red-necked Amazon *Amazona arausiaca*	^{b} .5	.044	.9	.61	2.6	.076	.17	2.2	13	14	38	.035	.92	4.6	58
Painted Tody-flycatcher *Todirostrum pictum*	$^{b:d}$ .0069	.14	1	.64	3.2	.048	.049	1	1.8	1.8	6.9	.22	.45	4.9	8.9
Verdin *Auriparus flaviceps*	$^{b:d:e:wq}$ .0069	^{d} .12	^{d} .98	.49	.91	^{d} .038	.035	^{e} 1	1.5	1.5	^{d} 5.6	.24	.34	$^{d:e:i}$ 5.5	8.3
Iberian Chiffchaff *Phylloscopus ibericus*	$^{b:d}$ .0082	^{d} .098	.93	.51	1.1	^{d} .038	^{d} .041	^{d} 1	1.6	1.6	^{d} 8	.15	.36	^{d} 8.3	13
Rufous-brown Solitaire *Cichlopsis leucogenys*	$^{b:d:wr}$ .048	.079	.84	.5	.95	.036	.04	.99	2.3	2.3	12	.11	.56	7.7	18

Table 4: Growth and demography for 20 randomly chosen mammals and birds. Estimator levels: data (black), genus (blue), family (green), order (yellow), and class (red). The superscript letters for data refer to references in the SI on data references.

level. The corresponding values are 99%, 86%, 99%, 99%, 98%, and 96% for mammals, where 42%, 22%, 45%, 41%, 36%, and 45% of the estimates are data.

For mass-specific metabolism 5% and 15% of the estimates for birds and mammals are data, and 84% and 95% of the estimates are at or below the family level. For $t_r = 1/q_{ad}$, 8% and 4% of the estimates for birds and mammals are data, and 88% and 77% are at or below the family level. The mass at birth ($\acute{w}_0$) and weaning ($\acute{w}_j$) have a strong data base in mammals (37% & 21% are data), but less so in birds especially for mass at fledging (7% & 2% are data).

Traits that are less supported by data are typically calculated from at least two independent parameters, with estimator levels given by the parameter that is estimated at the highest taxonomic level. These traits include ϵ, α, R, l_m, ϵ_n, I, and t_g. Yet, even net energy (ϵ) and resource handling (α)—which are calculated from seven underlying parameters—have 32% and 44% of the estimates in birds and mammals at or below the family level.

The estimated life history variation is plotted as allometric functions of body mass for birds and placentals in Fig. 3 and marsupials and bats in Fig. 4. The non-crossing black lines in the plots connect data, forming trees that illustrate the parameter space of the data. The estimated parameters for individual species are plotted by dots, with the taxonomic level of the estimator indicated by colour. The dots and lines show that the extrapolation of parameters across species are con-

Trait	w	α	$\underline{\beta}$	β	ϵ	$\acute{\epsilon}_g$	N	b	ϵ_n	h	h_o	v	I
Unit	kg	J	$\frac{W}{kg}$	$\frac{W}{kg}$	W	-	km^{-2}	$\frac{kg}{km^2}$	$\frac{W}{km^2}$	km^2	-	-	-
Striped Bandicoot *Microperoryctes longicauda*	$^{a:c:d:wq:ws}$ .53	.023	2.6	9.5	.22	23	87	46	450	.022	2	46	90
Bunyoro Rabbit *Poelagus marjorita*	$^{a:c:d}$ 2.5	1.2	3.1	6.1	7.4	2.6	54	140	1000	.13	6.8	27	190
Nelsons Spiny Pocket Mouse *Heteromys nelsoni*	$^{a:c:d}$ .063	.0078	6.6	23	.18	8.6	780	49	1200	.0026	2	110	230
Lesser Egyptian Jerboa *Jaculus jaculus*	$^{a:c:d:e}$ .057	.01	$^{c:e:f}$ 6.8	23	.23	6.2	620	35	900	.0039	2.4	89	220
Ash-gray Mouse *Pseudomys albocinereus*	$^{a:c:d}$ .03	.0053	8	27	.14	6.1	740	22	650	.014	10	40	410
Hoffmanns Sulawesi Rat *Rattus hoffmanni*	^{a} .15	.084	4.6	16	1.3	2.2	1500	220	4600	.0021	3.2	130	420
Small-footed White-toothed Shrew *Crocidura parvipes*	-	-	-	-	-	-	-	-	-	-	-	-	-
Sri Lankan Shrew *Suncus fellowesgordoni*	^{d} .0023	.00038	21	42	.016	6.7	1500	3.5	160	.00023	.35	130	47
Guinean Horseshoe Bat *Rhinolophus guineensis*	^{d} .012	.00045	8.2	32	.015	28	22	.27	8.9	.69	15	4.3	66
Ryukyu Long-fingered Bat *Miniopterus fuscus*	$^{a:d}$ .011	.00011	11	44	.0049	26	23	.25	3	.62	14	5.8	84
Chocolate Pipistrelle *Hypsugo affinis*	^{d} .0084	.00059	7.7	30	.018	15	5.6	.047	1.5	1	5.8	2.7	16
Long-tailed Pangolin *Phataginus tetradactylus*	$^{a:c:d}$ 2.5	1	^{f} .89	2.4	2.4	3	40	100	300	3.6	140	2.1	290
Nyala *Tragelaphus angasii*	$^{a:c:d:e}$ 99	28	2	3.7	110	4	$^{c:j:ad}$ 45	4400	19000	11	490	11	5500
Western Ornate Fruit-dove *Ptilinopus ornatus*	$^{b:d:wq}$ .11	.014	5.4	11	.15	8.8	31	3.6	42	3.2	99	2.1	210
Ashy Woodpecker *Mulleripicus fulvus*	^{b} .31	.05	9.7	12	.61	6.7	3.8	1.2	16	2.5	9.7	4.2	41
Red-necked Amazon *Amazona arausiaca*	^{b} .5	.094	5.4	11	1	5.8	3.8	1.9	22	.057	.22	31	6.8
Painted Tody-flycatcher *Todirostrum pictum*	$^{b:d}$ .0069	.0002	20	57	.011	35	^{ad} 7	.048	2.8	.012	.086	42	3.7
Verdin *Auriparus flaviceps*	$^{b:d:e:wq}$ .0069	.00042	$^{g:wq}$ 24	68	.028	17	180	1.2	86	.015	2.7	46	120
Iberian Chiffchaff *Phylloscopus ibericus*	$^{b:d}$ .0082	.00075	20	56	.042	11	43	.35	20	.032	1.4	28	39
Rufous-brown Solitaire *Cichlopsis leucogenys*	$^{b:d:wr}$ .048	.0053	14	26	.14	9.6	30	1.4	40	.11	3.2	17	57

Table 5: Energetics and population ecology for 20 randomly chosen mammals and birds. Estimator levels: data (black), genus (blue), family (green), order (yellow), and class (red). The superscript letters for data refer to references in the SI on data references.

tained within the overall parameter space of the data.

The general overlap between estimates and data holds especially for traits with many data, where the black trees cover almost the complete parameter space of the estimates. Yet, narrow extrapolation areas exist, like the line of order-level dots (yellow) for the allometric scaling of metabolism (β) in larger placentals. The parameters with fewer data have large data free areas that are dominated by especially order and family level estimators. But even these extrapolation areas tend to be contained within the space of scattered data.

3.2 Life history variation

Table 4 list the growth and demographic parameters, and Table 5 the energetic and population ecological parameters, for 20 randomly chosen species. The complete set with 11,188 models for birds, and 4,937 models for mammals, are listed in the SI. These estimates illustrate a wide diversity of life histories, with Table 6 summarising the median values of selected traits for birds, placentals (minus bats), marsupials, and bats (BPMB). Table 6 includes also estimates of the allometric intercepts presenting the expected traits of similar sized species of 1kg, and the 95% ranges of the inter-specific variation of the four taxa.

Body mass & net energy: The trait variation across and within the four taxa reflects underlying variation in the conditions of natural selection, with the selected inter-specific range in body mass covering 4.8,

Trait	w	ϵ	$\underline{\beta}$	α	m	t_m	t_r	q_{ad}	R	N	b	ϵ_n	h	h_o	ι
Unit	g	W	$\frac{\text{W}}{\text{kg}}$	J	y^{-1}	y	y	y^{-1}	t_r^{-1}	$\frac{1}{\text{km}^2}$	$\frac{\text{kg}}{\text{km}^2}$	$\frac{\text{W}}{\text{km}^2}$	km^2	-	-
Birds	$36^{1,000}_{2.2}$	$.086^{1.4}_{2.1}$	$13^{3.8}_{.93}$	$.0025^{0.17}_{2.8}$	$5.5^{3.9}_{.66}$	$1^{1.8}_{.57}$	$2.6^{4.7}_{.61}$	$.39^{0.21}_{.61}$	$14^{19}_{.61}$	$14^{3.8}_{2}$	$.69^{3.8}_{2.2}$	$23^{-}_{1.9}$	$.086^{3.5}_{3.1}$	$1.7^{13}_{2.9}$	$1^{-}_{1.9}$
Plac.	$150^{1,000}_{4}$	$.58^{2.1}_{3.1}$	$4.9^{3.5}_{1.1}$	$.038^{0.24}_{4.1}$	$7.1^{3.7}_{1.5}$	$.53^{0.92}_{1.4}$	$1.6^{2.9}_{.98}$	$.62^{0.34}_{.98}$	$13^{11}_{.73}$	$360^{57}_{3.6}$	$43^{57}_{2.5}$	$720^{-}_{2.5}$	$.0054^{0.074}_{4.7}$	$2.7^{4.2}_{2.6}$	$2.5^{-}_{2.1}$
Mars.	$320^{1,000}_{2.9}$	$1.1^{1.8}_{1.9}$	$3.1^{2.3}_{.83}$	$.1^{0.29}_{2.8}$	$5.3^{3}_{1.3}$	$.85^{0.97}_{.74}$	$1.5^{2.6}_{.68}$	$.66^{0.39}_{.68}$	$9^{7.9}_{.71}$	$110^{74}_{1.8}$	$23^{74}_{2.8}$	$360^{-}_{2.2}$	$.026^{0.048}_{2.8}$	$3.2^{3.5}_{2.7}$	$2.2^{-}_{2.2}$
Bats	$14^{1,000}_{1.8}$	$.019^{3.1}_{2.3}$	$7.7^{3}_{.53}$	$.0006^{0.13}_{2.4}$	$1.4^{1.1}_{.4}$	$.98^{2}_{.56}$	$3.6^{6.6}_{.33}$	$.28^{0.15}_{.33}$	$5.2^{7.2}_{.43}$	$18^{40}_{1.2}$	$.25^{40}_{2.6}$	$7.9^{-}_{2.5}$	$.82^{2.7}_{1.2}$	$13^{110}_{1.2}$	$1.5^{-}_{1.8}$

Table 6: Inter-specific medians of selected traits covering all models for birds, placentals (Plac.), marsupials (Mars.), and bats. Superscript values are allometric intercepts listing expected trait values for body masses of 1kg, and subscripts are the order of magnitudes of the 95% ranges of the inter-specific distributions (the latter calculated for $I = e^{\iota}$ for the level of interference).

7.9, 4, and 2.7 orders of magnitude for BPMB. The median marsupial is 113% larger than the median placental that is 317% larger than the median bird that is 157% larger than the median bat.

This body mass variation is selected primarily from underlying variation in net energy, where the population dynamic feedback selects net energy from reproduction to body mass—and vice versa—to maintain a constant level of interference competition in the population. This selection predicts the dependence of mass (w) on net energy (ϵ) as an allometric relation where $w \propto \epsilon^{4/3}$ (Witting 2017a), with the proportional relation being between body mass and net energy on the per-generation timescale of natural selection.

The $\epsilon^{4/3}/w$ ratios of the expected 95% range in body mass (calculated from the $\epsilon^{4/3}$ allometry given the 95% range in net energy) over the observed 95% body mass range are 1.22, 1.13, 0.81, and 1.68 for BPMB. This lack of a 100% match is expected because additional body mass variation is selected from allometrically uncorrelated variation in the survival of adults and offspring.

The efficiency by which a species allocates net energy into body mass is reflected in the w/ϵ ratio. The medians of this ratio are 0.42, 0.26, 0.29, and 0.74kg/W for BPMB, showing that bats are selected for a more efficient conversion of net energy to mass relative to the other taxa. Marsupials and birds are medium efficient, and placentals least efficient. We will take a closer look at reasons for these differences when we examine the demographic traits below but let us first examine how the different taxa generate net energy.

With the net energy of a species following from the $\epsilon = \alpha\beta$ product between resource handling (α) and metabolic pace (β), the inter-specific variation in net energy and body mass reflects underlying variation in resource handling and mass-specific metabolism. As mass-specific metabolism in birds and mammals approach Kleiber (1932) scaling with allometric exponents around $-1/4$, the 95% range of mass-specific metabolism should cover approximately 25% of the corresponding range in body mass. With the actual β/w ratios of the 95% range being 0.42, 0.28, 0.29, and 0.29 for BPMB this holds approximately for most taxa, except that the metabolic estimates for bats have more variation than expected from Kleiber scaling alone.

As the $-1/4$ power decline in mass-specific metabolism with an increase in mass is selected as a secondary mass-rescaling that is imposed by the selection of mass (Witting 2017a), the primary contributor to the selected variation in body mass is the underlying variation in resource handling, reflecting variation in the ways that species handle their resources as well as variation in the density of resources. This downscaling of mass-specific metabolism ($\beta \propto w^{-1/4}$) during the selection of mass generates a decline in net energy in physical time ($\epsilon = \alpha\beta \propto w^{-1/4}$ given constant α), but it maintains net energy on the per-generation timescale of natural selection ($\epsilon t_r \propto w^0$ given constant α) because it includes a corresponding dilation ($t_r \propto 1/\beta \propto w^{1/4}$) of natural selection time. Thus, when other things are equal, the body mass within a taxon is selected in proportion with resource handling ($w \propto \alpha$).

The dependence of mass on resource handling is reflected in the α/w ratio, with the ratios of the 95% ranges of the inter-specific distributions being 1.27, 1.02, 0.97, and 1.33 for BPMB. Except for birds, these ratios are closer to the other-things-being-equal-value of unity than the corresponding $\epsilon^{4/3}/w$ ratios for net energy given above. The larger α/w ratio for birds reflects—at least to some degree—a smaller (-0.33; Witting 2023) than expected ($-1/4$) allometric exponent for mass-specific metabolism. This stronger decline relative to Kleiber scaling implies an additional decline in the pace of handling with increased mass, implying a stronger than proportional dependence of mass on resource handling as the net energy that de-

fines mass is given by the $\alpha\beta$ product.

The stronger metabolic scaling in birds seems to reflect a diversification that increases as a taxon evolves through time (Witting 2018, 2023), with the primary selection of metabolism accelerating more in smaller species as they are selected over a larger number of generation than larger species. This deviation from a linear metabolic allometry is found also in terrestrial placentals (Kolokotrones et al. 2010), but not in marsupials which have close to perfect Kleiber scaling with an allometric exponent of -0.25 (MacKay 2011). This agrees with the above α/w ratio of unity for marsupials, while the close to unity value for placentals is confounded as it is a joint measure for both two-dimensional (2D) and three-dimensional (3D) ecological systems, with the estimated metabolic exponent of placentals being -0.29 for 2D and -0.14 for 3D (Witting 2023). With a metabolic exponent of -0.21, the large α/w ratio of 1.33 for bats does not reflect the allometric scaling of metabolism, although it may reflect the larger than expected amounts of metabolic variation in bats.

To examine the different ways the different taxa generate net energy, let us compare the median β/α ratios. These are 5200, 130, 31, and 13000/kg s for BPMB, which means that metabolic pace is much more important for the generation of net energy in bats and birds than in placentals and marsupials. If we correct for mass and compare the corresponding β/α ratios at the allometric intercept, we find a less extreme but similar ranking (22, 15, 7.9, & 23). The latter reflects a resource handling in bats and birds at 1kg that are only 54% and 71% of the corresponding resource handling in placentals, with mass-specific metabolism in birds and bats at 1kg being 109% and 86% of the corresponding metabolism in placentals. The low importance of metabolism for the generation of net energy in marsupials reflects both a mass-specific metabolism that is 66% of the metabolism in placentals at the 1kg intercept, and a marsupial resource handling at 1kg that is 121% of handling in placentals.

Demography: With demographic parameters like m, t_m, t_r, and q_{ad} being yearly rates or ages/periods they scale inversely with mass-specific metabolism with allometric exponents for terrestrial birds and mammals around 1/4 (Witting 1995, 2023). The 95% range of the inter-specific variation are thus as expected about similar to the corresponding range for mass-specific metabolism, with the ratio of the average range for m, t_m, and $t_r = 1/q_{ad}$ over β being 0.66, 1.2, 1.1, and 0.81 in BPMB.

The natural selection of an efficient conversion of net energy into body mass is to a large degree determined by the survival of offspring and adults. With body mass reflecting the available net energy per offspring, the efficiency is proportional to the $t_r\epsilon/R$ ratio of lifetime net energy ($t_r\epsilon$) over lifetime reproduction (R). And with lifetime reproduction being inversely related to the survival of offspring to maturity ($R = 2/l_m$ from $\lambda = l_m R/2 = 1$), and the reproductive period ($t_r = 1/q_{ad}$) being inversely related to adult mortality, the efficiency declines if offspring and/or adult mortality increases. A low offspring survival implies that more offspring are produced from the same amount of energy, and a low adult survival implies that less energy is available for the production of the number of offspring produced per lifetime.

These relationships are evident as contrasts in the life history differences between the four taxa. With median offspring survival (l_m) in bats being 219%, and median adult survival 162%, of the average median offspring and adult survival in birds, placentals, and marsupials, bats have by far the most efficient conversion of net energy to mass, with a median w/ϵ conversion ratio of 229% relative to the average median across the other three taxa. This is reflected in the lowest median lifetime reproduction of $5.2/t_r$, the longest median reproductive period of 3.6y, and the lowest median annual reproduction of 1.4/y.

Following bats, birds and marsupials have about similar median w/ϵ conversion efficiencies of 0.42 and 0.29kg/W, being on average 137% of the median efficiency of placentals. Yet, the ways of obtaining these median conversion efficiencies differ. Where adult bird survival is 179% of adult survival in marsupials at the median, the median survival of marsupial offspring to reproductive maturity is 157% of offspring survival in birds. This implies similar annual reproduction in the two taxa (medians of 5.5/y and 5.3/y), but a low median lifetime reproduction of $9/t_r$ in marsupials, compared with the largest lifetime reproduction of $14/t_r$ obtained by birds during their relatively long median reproductive period of 2.6y following low adult survival. Having low median adult survival like marsupials, and low median offspring survival like birds, placentals have the smallest efficiency when it comes to converting net energy into mass.

Ecology: For the ecological traits there are only few data for bats, and I will thus not include them in the comparison. For the remaining three taxa let us examine the 95% range for abundance (N), biomass (b), home range (h), and home range overlap (h_o) relative to the expected range from the variation in body mass

given the allometric relations $N \propto w^{-3/4}$, $b \propto w^{1/4}$, $h \propto w^1$, & $h_o \propto w^{1/4}$ (I do not include ϵ_n and ι as these are predicted invariant of w). These ratios show that the average observed range in N, b, h, and h_o are 1.06, 1.91, 1.18, and 2.10 times the expected range. These numbers indicate a large overdispersal in b and h_o relative to the allometric expectations, which may reflect not only additional ecological variation but also increased estimation uncertainty for ecological traits.

When it comes to between taxa differences there is for most ecological traits a very large difference between birds and mammals (especially placentals). The median abundance, biomass, and resource consumption of placental populations are 26, 62, and 31 times the corresponding medians for birds, and the median home range of placentals is only 6.3% of the median of birds. These differences remain pronounced when corrected for mass, where the median intercepts for abundance and biomass in placentals are 15 times the medians for birds, while the median intercept for placental home range is only 2.1% of the median intercept in birds. These large ecological differences between birds and mammals are in sharp contrasts to the median home range overlap, which is essentially identical between the two taxa (1.7 in birds vs. 2.7 in placentals).

The relatively similar home range overlap in birds and mammals indicates that the spatial packing of home ranges plays a stable central role in the joint natural selection of the life histories and population dynamic ecology as a whole. This is in line with population dynamic feedback selection, where it is the density dependent trade-off between the local resource exploitation of individuals and the interactive competition between individuals that selects a home range overlap that optimises the individual foraging ecology, with the spatial dimensionality of the ecological packing of home ranges constraining the exponents of body mass allometries (Witting 1995, 2017a, 2023).

The level of interference competition that is selected by the spatial packing of home ranges is in fact the main selection attractor of population dynamic feedback selection, known as a competitive interaction fixpoint (Witting 1997). This attractor reflects a process where the population dynamic demography, density regulated abundance, and associated foraging ecology are feedback selected to a balance where they generate a level of interactive competition that is invariant of the selected body mass and pre-defined by the selection attractor of the competitive interaction fixpoint.

Dependent upon the overall constraints on the selection of mass, the level of interference competition at the competitive interaction fixpoint may differ (Witting 2002, 2008, 2017b). The ratio in the ι-level of interference for the selection attractor of an exponentially increasing body mass over the attractor of a stable mass, e.g., is $7/3 \approx 2.3$ given a two-dimensional packing of home ranges. This is close to the observed values of 2.5 and 2.2 for the placental/bird and marsupial/bird ratios of the median ι-estimates in Table 6.

Apart from the elevated interference competition—and associated increase in population abundance, biomass, and population energy consumption—that is necessary for the selection of an exponential increase in body mass, the feedback selection mechanisms for a stable and increasing body mass are similar selecting no obvious difference in the physiology and demographic traits (while differences are selected in the reproducing unit; Witting 2002). Hence, the median ecological differences, and relative demographic similarities, between birds and mammals (excluding bats) indicate that mammals are predominately selected for an increase in mass while birds are selected for a stable mass.

3.3 Population dynamics

The 16,125 equilibrium life history models provided by my study are easily extended into population dynamic simulations. This is exemplified in this section, where eight models are used to explain a diverse range of population dynamic timeseries.

The population dynamics of a species depend on the age-structured demography that defines the timescale of the dynamics, and on the population dynamic regulation that defines not only the bounds on abundance but also the properties of the dynamics, let it be monotonic growth, damped to stable population cycles, fluctuating, or chaotic dynamics.

While regulation is relatively easily estimated from timeseries of abundance estimates, this is not the case for the age-structured demography. It is thus essential that the latter is available from other sources, as the life history models provided in this paper. When these models are extended into age-structured population dynamic models with no regulation, they project a stable population in time.

Given widespread evidence for eco-evolutionary dynamics (e.g., Thompson 1998; Sinervo et al. 2000; Hairston et al. 2005; Coulson et al. 2011; Turcotte et al. 2011a,b; Bell 2017; Hendry 2017; Brunner et al. 2019), I include regulation by density dependent competition and regulation by population dynamic feedback selection, following Witting (2000, 2013). As described in Appendix C, this includes the addition of a density regulation parameter (γ) that regulates the growth rate

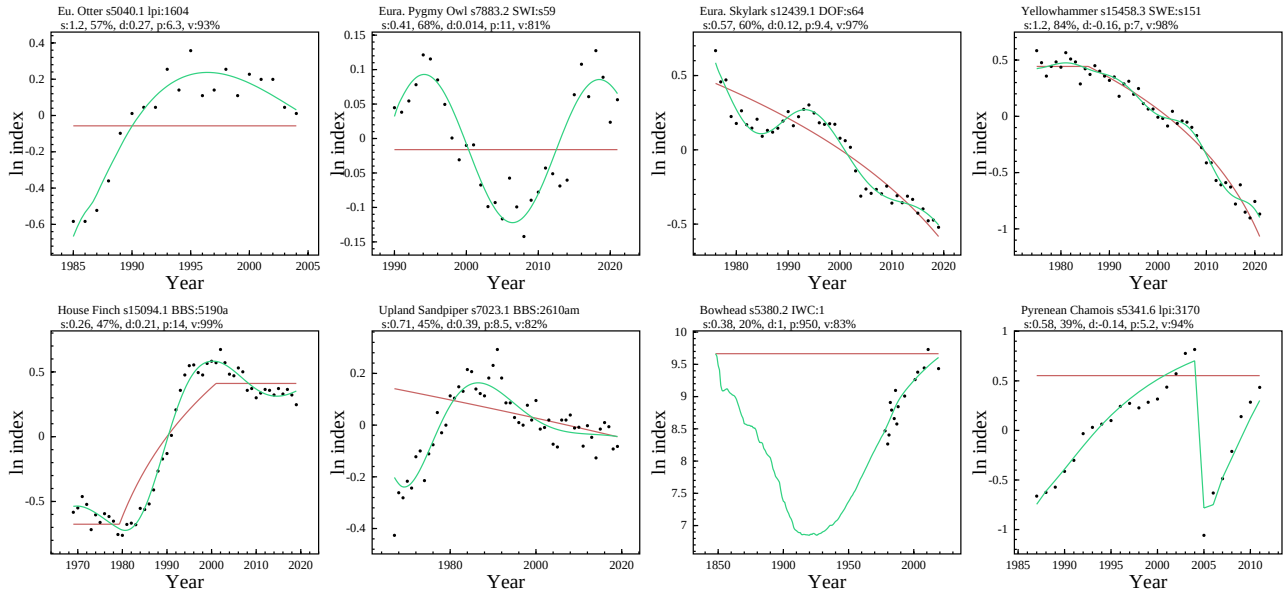

Figure 5: Examples of population dynamic models fitted to timeseries of abundance estimates (for details see the text). Dots are index series of abundance, red lines the estimated equilibria, and green curves the model trajectories. s:γ_ι & $\gamma_\iota/(\gamma_\iota+\gamma)$ in %; d:damping ratio; p:period in generations; v:explained variance.

as a function of the density dependent environment, and a selection regulation parameter (γ_ι) that accelerates the population dynamic growth below the equilibrium abundance and decelerates population growth above. Following Witting (2021), I use *i*) maximum likelihood statistics to estimate the two regulation parameters (and the equilibrium and initial abundance, as well as an initial measure of competitive quality) and *ii*) the Akaike information criterion (AIC, Akaike 1973) to determine if there is additional evidence for a change in equilibrium abundance or catastrophic mortality in a specific year.

The eight examples of fits to timeseries of abundance estimates are shown in Fig. 5. For these, I estimate that about 20% to 80% of total regulation is caused by selection, as measured by the $\gamma_\iota/(\gamma+\gamma_\iota)$ ratio. This generates a cyclic/over-compensatory dynamics that cannot be explained by density regulation alone. The over-compensation is illustrated by the growth of European Otter (*Lutra lutra*, from Sulkava 2006; LPI 2022) in Finland. The Eurasian Pygmy Owl (*Glaucidium passerinum*, from Knaus and Schmid 2022) in Switzerland illustrates that populations that are both density and selection regulated have the ability to decline for longer periods below the equilibrium abundance, and to increase for longer periods above the equilibrium. Pure density regulated populations will typically only decline above the equilibrium and increase below.

Many birds that live in the farmlands of Europe have declined more or less continuously since systematic monitoring was established in several countries in the 1970th and 1980th (Gregory et al. 2019; PECBMS 2022). This is illustrated by Eurasian Skylarks (*Alauda arvensis*, from DOF 2022) in Denmark and Yellowhammers (*Emberiza citrinella*, from SFT 2022) in Sweden. The best AIC-selected models estimate that Skylark habitats in Denmark and Yellowhammer habitats in Sweden have fragmented and deteriorated by 64% and 80% since the middle of the 1970th.

Where many species suffer, others benefit from habitat changes imposed by humans. Being originally a bird of the western Unites States and Mexico, House Finches (*Haemorhous mexicanus*) established themselves in human-altered habitats throughout the Unites States and southern Canada following a small release on Long Island in the 1940th. Across the mid-west the population was relatively stable from 1970 to 1980, followed by a large increase driven by a three-fold increase in equilibrium (most likely expansion into new habitats), according to the best AIC selected model run on data compiled (Witting 2021) from BBS (2022).

A strong population increase need not necessarily reflect improved conditions. Being a grassland species native to the prairies of Unites States and Canada, the Upland Sandpiper (*Bartramia longicauda*) is another species that is vulnerable to habitats lost to agriculture

with an increased use of pesticides. Based on the best AIC selected model run on BBS (2022) data compiled by Witting (2021), from about 1970 to 1990 Upland Sandpipers recovered by an increase of about 50% from a low abundance. Yet, the estimated habitat conditions deteriorated by about 20% from 1970 to 2020, with the species declining by about 20% from 1990 to 2020.

A longstanding threat to many species is direct anthropogenic removals, with commercial whaling in past centuries causing some of the largest perturbations of natural populations worldwide. The population modelling of these perturbations subtracts the historical catches from the simulated population, fitting the model trajectory to a relatively short timeseries of recent abundance estimate (Punt and Butterworth 1999; Wade 2002; Witting 2013). The bowhead whale (*Balaena mysticetus*) in the Bering-Chukchi-Beaufort Seas is one example, where the fitted model estimates that the historical catches of about $21,000$ bowheads from 1850 to 1950 (data from https://iwc.int) caused a collapse to about 1000 individuals in 1920, less than 7% of the pre-whaling abundance. From about 1910 to 1930 there was a turning point where reduced catches and increased growth (from the relaxed density regulation and selection acceleration of the depleted population) turned the population decline into an increase. With bowheads being reproductively mature around 23 years of age, it took approximately 100 years to recover to the pre-whaling abundance of about $15,000$ whales, with todays population continuing to increase.

Population perturbations may also be imposed by natural causes. The Spanish population of Pyrenean Chamois (*Rupicapra pyrenaica*) in Cerdanya-Alt Urgell increased steadily until 2005, where approximately 3,000 died from a border disease virus infection (Marco et al. 2009; data from Lopez-Martin et al. 2013; LPI 2022). This caused the population to collapse by about 80% in a single year. Yet, with Chamois being reproductively mature at about 2 years of age the population was almost recovered by 2011.

4 Discussion

Based on 110,105 life history data from 614 literature sources, I used allometric extrapolations at the lowest taxonomic level with data to estimate population dynamic equilibrium life history models for 16,125 species of birds and mammals. With each model having 27 parameters, 435,375 life history and ecological traits were estimated in total. This includes estimates of metabolism, resource handling, net assimilated energy, individual growth, mortality, fecundity, age of reproductive maturity, generation time, life span, home range, population density, home range overlap, biomass, population consumption, and a relative measure of intra-specific interactive competition.

A cross validation of estimates against data confirmed the general absence of estimation bias (Fig. 1), with both allometrically correlated and uncorrelated variation captured by the estimated life history models (Section 3.2). Yet, as the majority of the estimated traits are inter-specific extrapolations, and as the underlying data come from many sources, it is essential to keep in mind the uneven distribution of uncertainties. This is captured to some degree by the removal of outlier data, filter-adjustment of unlikely values, and a colour coding of estimates that reflects the phylogenetic levels of the inter-specific extrapolation, with a separate uncertainty cv calculated for each entry in the trait x estimation-level matrix (Table 3).

Given these limitations, the value of having complete population dynamic life history models for 16,125 species of birds and mammals should not be underestimated. Validated data should always be preferred over model estimates, but life history data are incomplete or missing for most species, and complete life history and population dynamic models are needed in many cases.

By aligning my life history estimates with the energy flow in population dynamic feedback selection, it is possible to analyse the life history and population ecological variation in birds and mammals for a better understanding of the natural selection causalities that have created the observed variation. This is illustrated in Section 3.2, where the intra- and inter-taxon variation in birds, placentals, marsupials, and bats are described primarily by the natural selection consequences of variation in resource handling, metabolism, mortality, home range, and abundance. An essential finding suggests that birds are predominately selected for stable body masses, while mammals are predominantly selected for body masses that increase exponentially on evolutionary timescales.

Another example is Witting (2023), where the life history estimates are used to illustrate the natural selection causalities behind the body mass allometries in mammals and birds. This identifies not only the predominant Kleiber scaling, but also allometric deviations imposed by additional variation in mortality and the primary selection of metabolism through time.

The application of the estimated models is not restricted to evolutionary analyse. Another main reason for their development is illustrated in Section 3.3, which shows how the models are easy to extend into complete population dynamic simulations. These ex-

amples show how a diverse range of population dynamic timeseries are explained by the addition of population dynamic feedback selection on top of traditional density regulated models. A next step is the estimation of complete population dynamic models across thousands of population dynamic timeseries, allowing for a quantification of the relative importance of regulation by density dependence and natural selection. This is needed for the construction of a freely accessible library of Bird and Mammal Populations (https://mrLife.org/bmp.htm) allowing for online population dynamic analyses of all species.

5 Supplementary Information

si_inflection.pdf: Data fits of Richards growth curves;

si_outlier.pdf: Removal of outlier data;

si_filter.pdf: Four estimation filters;

si_bird_demo.pdf: Bird demography;

si_bird_energy.pdf: Bird energy/ecology;

si_mammal_demo.pdf: Mammal demography;

si_mammal_energy.pdf: Mammal energy/ecology;

si_ref.pdf: Data references.

Acknowledgements

I am grateful to those that collect and published life history and population dynamic data, and to reviewers who improved my study.

References

Akaike H. (1973). Information theory as an extension of the maximum likelihood principle. In: Petrov B. N. Csaki F. (eds). Second International Symposium on Information Theory: Akademiai Kiado, pp 267–281.

BBS (2022). EESC Breding Bird Survey. https://www.mbr-pwrc.usgs.gov/bbs/bbs.html.

Bell G. (2017). Evolutionary rescue. Ann. Rev. Ecol. Evol. Syst. 48:605–627.

BirdLife (2022). HBW and BirdLife Taxonomic Checklist v7. BirdLife International, datazone.birdlife.org.

Brown J. H., Gillooly A. P., Allen V. M., Savage G. B. (2004). Towards a metabolic theory of ecology. Ecology 85:1771–1789.

Brown J. H. Sibly R. M. (2006). Life-history evolution under a production constraint. Proc. Nat. Acad. Sci. 103:17595–17599.

Brunner F. S., Deere J. A., Egas M., Eizaguirre C., Raeymaekers J. A. M. (2019). The diversity of eco-evolutionary dynamics: Comparing the feedbacks between ecology and evolution across scales. Funct. Ecol. 33:7–12.

Charlesworth B. (1980). Evolution in age-structured populations. Cambridge University Press, Cambridge.

Charnov E. L. (1993). Life history invariants. Some explorations of symmetry in evolutionary ecology. Oxford University Press, New York.

Christiansen F. B. (1991). On conditions for evolutionary stability for a continuously varying character. Am. Nat. 138:37–50.

Coulson T., Macnulty D. R., Stahler D. R., Vonholdt B., Wayne R. K., Smith D. W. (2011). Modeling Effects of Environmental Change on Wolf Population Dynamics, Trait Evolution, and Life History. Science 334:1275–1278.

Damuth J. (1981). Population density and body size in mammals. Nature 290:699–700.

Damuth J. (1987). Interspecific allometry of population density in mammals and other animals: the independence of body mass and population energy-use. Biol. J. Linnean Society. 31:193–246.

De Magalhães J. P. Costa J. (2009). A database of vertebrate longevity records and their relation to other life-history traits. J. Evol. Biol. 22:1770–1774.

del Hoyo, J., Elliot, A., Sargatal, J., & Christie, D. A., eds (1992–2011). Handbook of the birds of the world. Vol. 1–16. Lynx Edicions, Barcelona.

DeSante D. F. Kaschube D. R. (2009). The monitoring avian productivity and survivorship (MAPS) program 2004, 2005, and 2006 report. Bird Pop. 9:86–169.

DOF (2022). Dansk Ornitologisk Forening. Punkttællinger. https://www.dof.dk.

Dunning J. B. (2007). Handbook of Avian Body Masses (2nd ed). CRC Press, Boca Raton.

Eshel I. Motro U. (1981). Kin selection and strong evolutionary stability of mutual help. Theor. Pop. Biol. 19:420–433.

Fenchel T. (1974). Intrinsic rate of natural increase: The relationship with body size. Oecologia 14:317–326.

Gompertz B. (1832). On the Nature of the Function Expressive of the Law of Human Mortality, and on a New Mode of Determining the Value of Life Contingencies. Phil. Trans. R. Soc. Lond. 123:513–585.

Gregory R. D., Skorpilova J., Vorisek P., Butler S. (2019). An analysis of trends, uncertainty and species selection shows contrasting trends of widespread forest and farmland birds in Europe. Ecol. Indic. 103:676–687.

Griffiths D. (1977). Caloric variation in Crustacea and other animals. J. Anim. Ecol. 46:593–605.

Hairston N. G. J., Ellner S. P., Geber M. A., Yoshida T., Fox J. A. (2005). Rapid evolution and the convergence of ecological and evolutionary time. Ecol. Lett. 8:1114–1127.

Hardy I. C. W. Briffa M. (2013). Animal contests. Cambridge University Press, Cambridge.

Hendry A. P. (2017). Eco-evolutionary dynamics. Princeton University Press, Princeton.

Herberstein M. E., McLean D. J., Lowe1 E., Wolff J. O., Khan K., Smith K., Allen A. P., Bulbert M., Buzatto B. A., Eldridge M. D. B., Falster D., Winzer L. F., Griffith S. C., Madin J. S., Narendra A., Westoby M., Whiting M. J., Wright I. J., Carthey A. J. R. (2022). AnimalTraits – a curated animal trait database for body mass, metabolic rate and brain size. Sci. Data 9:265.

Hudson L. N., Isaac N. J. B., Reuman D. C. (2013). The relationship between body mass and field metabolic rate among individual birds and mammals. J. Anim. Ecol. 82:1009–1020.

Jetz W., Sekercioglu C. H., Böhning-Gaese K. (2008). The worldwide variation in avian clutch size across species and space. PLOS Biol. 6:e303.

Johansson Ö., Ausilio G., Low M., Lkhagvajav P., Weckworth B., Sharma K. (2021). The timing of breeding and independence for snow leopard females and their cubs. Mamm. Biol. 101:173–180.

Jones K. E., Bielby J., Cardillo M., Fritz S. A., O'Dell J., Orme C. D. L., Safi K., Sechrest W., Boakes E. H., Carbone C., Connolly C., Cutts M. J., Foster K. J., Grenyer R., Habib M., Plaster C. A., Price S. A., Rigby E. A., Rist J., Teacher A., Binninda-Emonds O. R. P., Gittleman J. L., Mace G. M., Purvia A. (2009). PanTHERIA: a species-level database of life history, ecology, and geography of extant and recently extinct mammals. Ecology 90:2648.

Kleiber M. (1932). Body and size and metabolism. Hilgardia 6:315–353.

Knaus P., Schmid H., Strebel N., Sattler T. (2022). The State of Birds in Switzerland 2022 online. http://www.vogelwarte.ch.

Kolokotrones T., Savage V., Deeds E. J., Fontana W. (2010). Curvature in metabolic scaling. Nature 464:753–756.

Lemaitre J. F., Ronget v., Tidiere M., Allaine D., Berger V., Cohas A., Colchero F., Conde D. A., Garratt M., Liker A., Marais G. A. B., Scheuerlein A., Szekely T., Gaillard J. M. (2020). Sex differences in adult lifespan and aging rates of mortality across wild mammals. Proc. Nat. Acad. Sci. 117:8546–8553.

Leung B., Hargreaves A. L., Greenberg D. A., McGill B., Dornelas M., Freeman R. (2020). Clustered versus catastrophic global vertebrate declines. Nature 588:267–273.

Lloyd D. G. (1987). Selection of offspring size at independence and other size-versus-number strategies. Am. Nat. 129:800–817.

Lopez-Martin J. M., Casanovas R., Garcia-Petit J., Xifra J., Curia J., Canut J. (2013). Estatus y gestion del sarrio en el Pirineo catalan. In: Herrero J., Escuderi E., deLuco D. F., Garcia-Gonzalez R. (eds). El Sarrio Pirenaico Rupicapra p. pyrenaica: Biologia, Patologia Y Gestion: Publicaciones del Consejo de Proteccion de la Naturaleza de Aragon, pp 43–53.

LPI (2022). Living Planet Index database. www.livingplanetindex.org.

MacKay N. J. (2011). Mass scale and curvature in metabolic scaling. J. theor. Biol. 280:194–196.

Mahoney S. A. Jehl J. R. J. (1984). Body water content in marine birds. The Condor 86:208–209.

Marco I., Rosell R., Cabezon O., Mentaberre G., Casas E., Velarde R., Lavin S. (2009). Border disease virus among Chamois, Spain. Emerg. Inf. Diseases 15:448–450.

Maynard Smith J. (1971). The origin and maintenance of sex. In: Williams G. C. (ed). Group selection: Aldine Atherton, Chicago, pp 163–175.

Maynard Smith J. (1982). Evolution and the theory of games. Cambridge University Press, Cambridge.

Maynard Smith J. Price G. R. (1973). The logic of animal conflict. Nature 246:15–18.

McCarthy M. A., Citroen R., McCall S. C. (2008). Allometric scaling and Bayesian priors for annual survival of birds and mammals. Am. Nat. 172:216–222.

McKechnie A. E. Wolf B. O. (2004). The allometry of avian basal metabolic rate: Good predictions need good data. Physiolo Biochem Zool 77:502–521.

McNab B. K. (2008). An analysis of the factors that influence the level and scaling of mammalian BMR. Comp. Bioch. Physiol. A 151:5–28.

MDD (2023). Mammal Diversity Database (Version 1.11) [Data set]. Zenodo.org DOI:10.5281/zenodo.7830771.

Millar J. S., Burkholder D. A. L., Lang T. L. (1986). Estimating age at independence in small mammals. Can. J. Zool. 64:910–913.

Myhrvold N. P., Baldridge E. amd Chan B., Sivam D., Freeman D. L., Ernest S. K. M. (2015). An amniote life-history database to perform comparative analyses with birds, mammals, and reltiles. Ecology 96:3109.

Nasrinpour H. R., Reimer A. A., Friesen M. R., McLeod R. D. (2017). Data preparation for West Nile Virus agent-based modelling: protocol for processing bird population estimates and incorporating ArcMap in AnyLogic. JMIR Res Protoc 6:e138.

Odum E. P., Marshall S. G., Marples T. G. (1965). The caloric content of migrating birds. Ecology 46:901–904.

Parker G. A. (1974). Assessment strategy and the evolution of fighting behaviour. J. theor. Biol. 47:223–243.

PECBMS (2022). Pan-European Common Bird Monitoring Scheme. https://pecbms.info.

Prothero J. W. (2015). The design of mammals. A scaling approach. Cambridge University Press, Cambridge.

Punt A. E. Butterworth D. S. (1999). On assessment of the Bering-Chukchi-Beaufort Seas stock of bowhead whales (*Balaena mysticetus*) using a Bayesian approach. J. Cetacean Res. Manage. 1:53–71.

Richards F. J. (1959). A flexible growth function for empirical use. J. Exp. Bot. 10:290–300.

Ricklefs R. E. (2010). Embryo growth rates in birds and mammals. Funct. Ecol. 24:588–596.

Ricklefs R. E., Tsunekage T., Shea R. E. (2011). Annual adult survival in several new world passerine birds based on age ratios in museum collections. J. Ornithol. 152:481–495.

Roff D. A. (1992). The evolution of life histories. Theory and analysis. University of Chicago Press, New York.

Santini L., Isaac N. J. B., Ficetola G. F. (2018). TetraDENSITY: A database of population density estmates in terrestrial vertebrates. Global Ecol. Biog. 27:787–791.

SFT (2022). Svensk Fågeltaxering. http://www.fageltaxering.lu.se.

Sinervo B., Svensson E., Comendant T. (2000). Density cycles and an offspring quantity and quality game driven by natural selection. Nature 406:985–988.

Smith C. C. Fretwell S. D. (1974). The optimal balance between size and number of offspring. Am. Nat. 108:499–506.

Smith F. A., Brown J. H., Haskell J. P., Alroy J., Charnov E. L., Dayan T., Enquist B. J., Ernest S. K. M., Hadly E. A., Jablonski D., Jones K. E., Kaufman D. M., Lyons S. K., Marquet P., Maurer B. A., Niklas K., Porter W., Roy K., Tiffney B., Willig M. R. (2004). Similarity of mammalian body size across the taxonomic hierarchy and across space and time. Am. Nat. 163:672–691.

Stearns S. C. (1992). The evolution of life histories. Oxford University Press, Oxford.

Sulkava R. (2006). Ecology of the otter (Lutra lutra) in central Finland and methods for estimating the densities of populations. University of Joensuu, Biology PhD dissertation 0043.

Tamburello N., Cote I. M., Dulvy N. K. (2015). Energy and the scaling of animal space use. Amazoniana 186:196–211.

Taylor P. D. (1989). Evolutionary stability in one-parameter models under weak selection. Theor. Pop. Biol. 36:125–143.

Thompson J. N. (1998). Rapid evolution as an ecological process. Trends Ecol. Evol. 13:329–332.

Tobias J. A., Sheard C., Pigot A. L., et a. (2021). AVONET: morphological, ecological and geographical data for all birds. Ecol. Lett. 25:581–597.

Tucker M. A., Ord T. J., Rogers T. L. (2014). Evolutionary predictors of mammalian home range size: body mass, diet and the environment. Global Ecol. Biog. 23:1105–1114.

Turcotte M. M., Reznick D. N., Hare J. D. (2011a). The impact of rapid evolution on population dynamics in the wild: experimental test of eco-evolutionary dynamics. Ecol. Lett. 14:1084–1092.

Turcotte M. M., Reznick D. N., Hare J. D. (2011b). Experimental assessment of the impact of rapid evolution on population dynamics. Evol. Ecol. Res. 13:113–131.

Wade P. R. (2002). A Bayesian stock assessment of the Eastern pacific gray whale using abundance and harvest data from 1967–1996. J. Cetacean Res. Manage. 4:85–98.

Weisbecker V., Ashwell K., Fisher D. (2013). An improved body mass dataset for the study of Marsupial brain size evolution. Brain Behav. Evol. 13:81–82.

West G. B., Brown J. H., Enquist B. J. (1997). A general model for the origin of allometric scaling laws in biology. Science 276:122–126.

West G. B., Brown J. H., Enquist B. J. (1999). The fourth dimension of life: fractal geometry and allometric scaling of organisms. Science 284:1677–1679.

Williams G. C. (1975). Sex and evolution. Princeton University Press, Princeton.

Wilson, D. E. & Mittermeier, R. A., eds (2009–2014). Handbook of the mammals of the world. Vol. 1–4. Lynx Edicions, Barcelona.

Witting L. (1995). The body mass allometries as evolutionarily determined by the foraging of mobile organisms. J. theor. Biol. 177:129–137, https://doi.org/10.1006/jtbi.1995.0231.

Witting L. (1997). A general theory of evolution. By means of selection by density dependent competitive interactions. Peregrine Publisher, Århus, 330 pp, URL https://mrLife.org.

Witting L. (2000). Population cycles caused by selection by density dependent competitive interactions. Bull. Math. Biol. 62:1109–1136, https://doi.org/10.1006/bulm.2000.0200.

Witting L. (2002). From asexual to eusocial reproduction by multilevel selection by density dependent competitive interactions. Theor. Pop. Biol. 61:171–195, https://doi.org/10.1006/tpbi.2001.1561.

Witting L. (2007). Behavioural interactions selecting for symmetry and asymmetry in sexual reproductive systems of eusocial species. Bull. Math. Biol. 69:1167–1198, https://doi.org/10.1007/s11538–006–9112–x.

Witting L. (2008). Inevitable evolution: back to *The Origin* and beyond the 20th Century paradigm of contingent evolution by historical natural selection. Biol. Rev. 83:259–294, https://doi.org/10.1111/j.1469–185X.2008.00043.x.

Witting L. (2013). Selection-delayed population dynamics in baleen whales and beyond. Pop. Ecol. 55:377–401, https://dx.doi.org/10.1007/s10144–013–0370–9.

Witting L. (2017a). The natural selection of metabolism

and mass selects allometric transitions from prokaryotes to mammals. Theor. Pop. Biol. 117:23–42, https://dx.doi.org/10.1016/j.tpb.2017.08.005.

Witting L. (2017b). The natural selection of metabolism and mass selects lifeforms from viruses to multicellular animals. Ecol. Evol. 7:9098–9118, https://dx.doi.org/10.1002/ece3.3432.

Witting L. (2018). The natural selection of metabolism explains curvature in allometric scaling. Oikos 127:991–1000, https://dx.doi.org/10.1111/oik.05041.

Witting L. (2020). The natural selection of metabolism explains curvature in fossil body mass evolution. Evol. Biol. 47:56–75, https://dx.doi.org/10.1007/s11692–020–09493–y.

Witting L. (2021). Selection-regulated population dynamic in birds and mammals. Preprint at bioRxiv https://dx.doi.org/10.1101/2021.11.27.470201.

Witting L. (2023). On the natural selection of body mass allometries. Acta Oecol. 118:103889, https//dx.doi.org/10.1016/j.actao.2023.103889.

Appendix

A Demography

I estimate the demography of stable populations with a per-generation growth rate of unity

$$\lambda = l_m R/2 = 1 \tag{10}$$

with l_m being the probability that a newborn survives to the age of maturity, and R is the expected lifetime reproduction of females that survives to t_m, assuming an even sex ratio.

While data on age structured reproduction and survival are becoming increasingly available (e.g., Lemaitre et al. 2020), structured estimates are most often not available, and I estimate lifetime reproduction as a product

$$R = t_r m \tag{11}$$

where t_r is the expected reproductive period and m the average annual birth rate.

With $l_a = \prod_{x=0}^{a-1} p_x$ being the survival curve over age (a), the expected reproductive period is calculated as a function of adult survival (p_{ad}), where

$$\begin{aligned} t_r &= \frac{\sum_{a=t_m}^{t_l}(a+1-t_m)(l_a - l_{a+1})}{\sum_{a=t_m}^{t_l} l_a - l_{a+1}} \\ &= \sum_{a=t_m}^{t_l} l_a/l_m = \sum_{a=t_m}^{t_l} p_{ad}^{a-t_m} \\ &\approx \sum_{i=0}^{\infty} p_{ad}^i = \frac{1}{1-p_{ad}} \end{aligned} \tag{12}$$

given constant adult survival.

Following Charlesworth (1980), a useful measure of generation time is mean reproductive age

$$t_g = \frac{\sum_{a=t_m}^{t_l} a\, m_a\, l_a}{\sum_{a=t_m}^{t_l} m_a\, l_a} \tag{13}$$

Given constant yearly reproduction (m) and constant adult survival (p_{ad}), generation time reduces to a function of the age of maturity and adult survival

$$\begin{aligned} t_g &= \frac{m\, l_m \sum_{a=t_m}^{t_l} a\, p_{ad}^{a-t_m}}{m\, l_m \sum_{a=t_m}^{t_l} p_{ad}^{a-t_m}} \\ &= t_m + \frac{\sum_{a=t_m}^{t_l}(a-t_m)p_{ad}^{a-t_m}}{\sum_{a=t_m}^{t_l} p_{ad}^{a-t_m}} \\ &\approx t_m + \frac{\sum_{i=0}^{\infty} i p_{ad}^i}{\sum_{i=0}^{\infty} p_{ad}^i} = t_m + \frac{p_{ad}}{1-p_{ad}} \end{aligned} \tag{14}$$

B Estimation sequence

To estimate life history traits for all species with body mass estimates, I used a sequence of calculation where data and missing parameter estimates are constrained by the underlying demography, growth and energetics. This estimation includes four filters (see filter SI) that use model constraints and data distributions to adjust unexpected estimates for lifespan, adult survival, gross energy, and the growth rated parameters $\acute{w}_0$, $\acute{w}_j$ and t_j.

I converted data on brood size (m_b), brood frequency (m_f) and/or brood interval (m_i) to yearly reproduction $(m = m_b m_f,\ m_f = 1/m_i)$; and data on sexual maturity (t_s) to reproductive maturity $(t_m = t_s + t_p)$. Data on total metabolism (βw) were transformed to metabolic rates per unit mass (β), and the ratio $(\beta/\underline{\beta})$ of field (β) over basal $(\underline{\beta})$ metabolism was calculated for all species with data on both. Mortality $(q_{ad} = 1 - p_{ad})$ data were calculated from survival rates (p_{ad}) to have two mirror estimates of all survival data.

Missing values were then estimated by inter-specific extrapolations for m, t_p, t_j, t_m, t_l, $\acute{w}_0$, $\acute{w}_j$, z, h, N, $\underline{\beta}$, $\beta/\underline{\beta}$, p_{ad} and q_{ad}. Missing values for field metabolism (β) were obtained from the $\beta/\underline{\beta}$-ratio and basal metabolism. Missing values for p_{ad} and q_{ad} were first estimated independently by allometric correlations on p_{ad} and q_{ad}, and adjusted afterwards to identical mirror values in order to avoid unrealistic estimates where $p_{ad} > 1 \wedge q_{ad} < 0$ or $p_{ad} < 0 \wedge q_{ad} > 1$. With

$\bar{p_{ad}}$ being the average survival rate for the two missing parameter estimates of p_{ad} and q_{ad}, the adjustment was done by setting $q_{ad} = 1 - p_{ad}$ for $\bar{p_{ad}} \leq 0.25$, by setting $p_{ad} = 1 - q_{ad}$ for $\bar{p_{ad}} \geq 0.75$, and by setting $p_{ad} = \bar{p_{ad}}$ and $q_{ad} = 1 - \bar{p_{ad}}$ for $0.25 < \bar{p_{ad}} < 0.75$.

A survival/mortality filter was constructed from an invariant $\acute{l}_m = l_m / p_{ad}^{t_m}$-ratio. As adult survival is larger than offspring and juvenile survival in most species, we expect the $\acute{l}_m$ ratio to be somewhat smaller than unity in nearly all species. From the $\acute{l}_m$ distributions across all species, I determined an upper limit on $\acute{l}_m$ of 0.8 for birds and 0.95 mammals. Then, as $l_m = 2/t_r m = 2(1 - p_{ad})/m$, we find that models with $\acute{l}_m$ ratios above these limits may have an estimate of the reproductive rate (m) that is too low, or an estimate of the reproductive age (t_m) that is too high, or an estimate of adult survival (p_{ad}) that is too low.

For species that failed to pass the survival filter (i.e., $\acute{l}_m > 0.8$ for birds; $\acute{l}_m > 0.95$ for mammals), I would fist examine for the possibility of outlier data for m and t_m. For this I would, for species with m and/or t_m data, estimate the corresponding missing parameter values for m and t_m. If one of the latter two estimates made the species pass the survival filter, I would classify the data value as an outlier. If no outlier was identified I would increase adult survival to obtain a $\acute{l}_m$ ratio that resembled the missing parameter estimate of $\acute{l}_m$ for that species. I would then remove the p_{ad} and q_{ad} outliers from the main data and rerun the complete estimation sequence until no extra outliers were identified.

Estimates were then calculated as $t_r = 1/(1 - p_{ad})$ by eqn 12, $t_g = t_m + p_{ad}/(1 - p_{ad})$ by eqn 13, $R = t_r m$, $l_r = p_{ad}^{t_r}$, and $l_m = 2/t_r m$ from zero growth $\lambda = l_m t_r m/2 = 1$ at equilibrium.

A lifespan filter adjusted unlikely small t_l values, and all growth related parameters $\acute{w}_0$, $\acute{w}_j$, and t_j were filtered for unexpected values. $\bar{w}_j$ was then estimated by eqn 6, net energy as $\epsilon = w_e \acute{\beta} R/t_r$, gross energy as $\epsilon_g = w\beta + \epsilon/2$ including the gross energy filter, resource handling as $\alpha = \epsilon/\beta$, home range overlap as $h_o = hN$, encounter rate as $v = \beta w^{1/2d}/h^{1/d}$, and the level of interference as $I = h_o v$ followed by a rescaling to set $\iota = \ln I$ equal to unity at the median across all birds.

C Population dynamics

The age-structured population dynamic model is parameterised from the age of reproductive maturity in years (t_m), annual reproduction (m), and annual survival (p_{ad}) of adults. These parameters are converted to an appropriate timescale where the timestep of the iteration is $\Delta t \leq \min(1, t_m)$, with parameters scaled as $a_m = t_m/\Delta t$, $m^* = m\Delta t$, and $p = {p_{ad}}^{1/\Delta t}$.

The survival parameter p is used as the survival rate for all age-classes except age-class zero. To calculate age-class zero survival, I converted p into the reproductive period $t_r = 1/(1 - p)$, to calculate lifetime reproduction $R = t_r m^*$, and $l_m = 2/R$ from the equilibrium constraint $l_m R/2 = 1$. Age class zero survival is then calculated as $p_0 = l_m p^{1-a_m}$.

With $x \gg a_m$ being the maximum lumped age-class, the number $n_{a,t}$ of individuals of age $0 < a < x$ at timestep t is

$$n_{a,t} = p_{a-1} n_{a-1,t-1} \tag{15}$$

and the number in age-class x

$$n_{x,t} = p_x n_{x,t-1} + p_{x-1} n_{x-1,t-1} \tag{16}$$

with $p_a = p_0$ for $a = 0$ and $p_a = p$ for $a \geq 1$. Let the number of individuals in each age-class relate to time just after each timestep transition, with offspring at t being produced by the $t - 1$ individuals that survive to the $t - 1 \rightarrow t$ transition, with the density dependent ecology being approximated by the average 1+ abundance of the two timesteps:

$$\hat{n}_t = 0.5 \sum_{a \geq 1} n_{a,t} + n_{a,t-1} \tag{17}$$

The number of offspring in age-class zero is then

$$n_{0,t} = 0.5\ m^* \left(\frac{\hat{n}^*}{\hat{n}_t} \right)^{\gamma} \sum_{a \geq a_m} \tilde{m}_{a,t}\ n_{a,t} \tag{18}$$

where γ is the strength of density regulation, and $\tilde{m}_{a,t} = 1/q_{a,t}$, with $q_{a,t}$ being the average competitive quality of cohort a at t. At the population dynamic equilibrium $q_a^* = 1$ for all ages. More generally $q_{a,t} = q_{a-1,t-1}$ and

$$q_{x,t} = \frac{q_{x,t-1} p_x n_{x,t-1} + q_{x-1,t-1} p_{x-1} n_{x-1,t-1}}{n_{x,t}} \tag{19}$$

assuming that there is no change in the quality of a cohort over time. The quality of offspring

$$q_{0,t} = \frac{\sum_{a \geq a_m} q_{a,t}\ n_{a,t}}{\sum_{a \geq a_m} n_{a,t}} \left(\frac{\hat{n}_t}{\hat{n}^*} \right)^{\gamma_\iota} \tag{20}$$

is the average quality of the mature component multiplied by the density dependent selection, with γ_ι being the selection response.

For the initial conditions of an iteration I use the same quality across all individuals, and an initial abundance with a stable age-structure

$$c_a = l_a / \sum_{a \geq 0} l_a \tag{21}$$

where $l_0 = 1$, $l_a = p_0\ p^{a-1}$ for $1 \leq a < x$, and $l_x = p_0\ p^{x-1}/(1 - p)$.